NACA TN 3383

NATIONAL ADVISORY COMMITTEE FOR AERONAUTICS

TECHNICAL NOTE 3383

INVESTIGATION OF THE TURBULENT BOUNDARY LAYER ON A YAWED FLAT PLATE

By Harry Ashkenas and Frederick R. Riddell

Cornell University

Washington

April 1955

NATIONAL ADVISORY COMMITTEE FOR AERONAUTICS

TECHNICAL NOTE 3383

INVESTIGATION OF THE TURBULENT BOUNDARY LAYER ON A YAWED FLAT PLATE

By Harry Ashkenas and Frederick R. Riddell

SUMMARY

The problem of the effect of yaw on the turbulent boundary layer and skin friction of infinite cylinders is reviewed and compared with the case of laminar flow. It is concluded that present understanding of the mechanism of turbulent shear does not permit extension of two-dimensional data even to this elementary case of three-dimensional flow.

Experiments carried out on three flat plates yawed 0°, 30°, and 45° with artificially fixed transition in a low-speed, low-turbulence tunnel are described. The effects of yaw on the velocity profile and on the direction of flow near the plate are found to be small. The boundary-layer displacement thickness on a yawed plate is found to grow in the streamwise direction at a rate slightly greater than it does on the unyawed plate; this is in contrast with the laminar case where the "independence principle" discovered by Prandtl and others leads to a substantially reduced rate of growth on yawed plates. It is also in conflict with the results of Young and Booth, who concluded from their experiments that the independence principle applied to turbulent flow. The work of Young and Booth is reviewed, and possible sources of the discrepancy are suggested.

INTRODUCTION

For laminar flow over a yawed infinite cylinder the boundary-layer equations for flow in the chordwise direction are independent of the spanwise flow (refs. 1 and 2). Hence, the chordwise flow can be calculated with no reference to the spanwise flow and the results then used to calculate the spanwise flow. This is sometimes called the "independence principle."

An investigation has been undertaken to determine the effects of yaw on the turbulent boundary-layer flow over a cylinder and, in particular, to ascertain whether such an independence principle also exists in the turbulent case. As an initial step the experiments have been

limited to the flat-plate case (i.e., the external pressure gradient is zero), the results of which are presented herein.

The fundamental difficulty in calculating the turbulent boundary layer, in even the simplest case, is the lack of knowledge of the relation between the Reynolds stresses and the mean velocity distributions. It is this lack of knowledge which makes it impossible to demonstrate (subject to the usual boundary-layer approximations) just what the effect of yaw will be for turbulent layers. Conversely, an experimental investigation of the effect of yaw casts some light on the relation between the turbulent stresses and the other flow quantities.

In the course of the experiments it was necessary to investigate quite closely the effectiveness of sandpaper roughening at the leading edge in producing an adequate turbulent boundary layer. These experimental results, together with those of Klebanoff and Diehl (ref. 3), should prove useful for other boundary-layer experiments.

The present investigation was conducted at Cornell University under the sponsorship and with the financial assistance of the National Advisory Committee for Aeronautics. The authors wish to express their appreciation to Profs. W. R. Sears and N. Rott for their encouragement and for their many valuable comments during the course of the investigation. The assistance of Messrs. J. Spencer, S. W. Liu, and H. Mirels in carrying out the experimental program is gratefully acknowledged.

SYMBOLS

H	shape parameter, δ^*/ϑ
p	static pressure
q	dynamic pressure
Re	Reynolds number
U,V,W	mean velocity components in x,y,z coordinates
$u,v,w,$	instantaneous velocity fluctuation components in x,y,z coordinates
x,y,z	coordinate system fixed to body (see fig. 1)
δ	boundary-layer thickness

δ^* displacement thickness, $\int_0^\delta \left(1 - \frac{U}{U_1}\right)dz$

ϑ momentum thickness, $\vartheta \equiv \vartheta_{uu} = \int_0^\delta \frac{U}{U_1}\left(1 - \frac{U}{U_1}\right)dz$

ϑ_{uv} mixed momentum thickness, $\int_0^\delta \frac{V}{U_1}\left(1 - \frac{U}{U_1}\right)dz$

Λ angle of yaw of leading edge

μ coefficient of viscosity

ν kinematic viscosity

ξ, η coordinate system defined by free-stream velocity (see fig. 2)

ρ density

τ shearing stress

τ_o shearing stress at wall

$( )_1$ refers to free-stream value

DEFINITION OF PROBLEM

Consider the laminar- and turbulent-boundary-layer equations for the two-dimensional body in the coordinate system of figure 1:

$$U \frac{\partial U}{\partial x} + W \frac{\partial U}{\partial z} = -\frac{1}{\rho}\frac{\partial p_1}{\partial x} + \frac{1}{\rho}\frac{\partial \tau_{xz}}{\partial z} \tag{1}$$

$$U \frac{\partial V}{\partial x} + W \frac{\partial V}{\partial z} = \frac{1}{\rho}\frac{\partial \tau_{yz}}{\partial z} \tag{2}$$

where for laminar flow

$$\left.\begin{aligned} \tau_{xz} &= \mu \frac{\partial U}{\partial z} \\ \tau_{yz} &= \mu \frac{\partial V}{\partial z} \end{aligned}\right\} \tag{3}$$

and for turbulent flow

$$\left.\begin{aligned} \tau_{xz} &= \mu \frac{\partial U}{\partial z} - \rho\overline{uw} \\ \tau_{yz} &= \mu \frac{\partial V}{\partial z} - \rho\overline{vw} \end{aligned}\right\} \tag{4}$$

The continuity equation for laminar flow is

$$\frac{\partial U}{\partial x} + \frac{\partial W}{\partial z} = 0 \tag{5}$$

and for turbulent flow is

$$\frac{\partial U}{\partial x} + \frac{\partial W}{\partial z} = 0 \tag{6}$$

together with

$$\frac{\partial u}{\partial x} + \frac{\partial v}{\partial y} + \frac{\partial w}{\partial z} = 0 \tag{7}$$

Equation (7) must be satisfied at each instant although, if a time mean is taken, it is identically satisfied.

A mathematical statement of the independence principle is that equation (1) for chordwise flow together with the appropriate continuity equation must be independent of the spanwise flow component V. Specifically, this can be stated as follows: τ_{xz} must be independent of V and of τ_{yz}. It can be seen at once that this is true for laminar flow. For turbulent flow, however, the condition to be satisfied is that $\overline{uw}$ must be independent of V and $\overline{vw}$. Since v varies with V and equation (7) must be instantaneously satisfied, this appears as a very complex requirement indeed. Hence, the experimental evidence of Young and Booth (ref. 4) that the independence principle does apply to turbulent flow is significant and rather surprising.

In this investigation the boundary-layer growth and the flow direction in the boundary layer[1] were measured on an unyawed flat plate and on flat plates yawed 30° and 45° with respect to the free stream.

A convenient basis for evaluating such measurements may be obtained by analogy with the known results for laminar flow (refs. 1 and 2) as follows:

Consider laminar flow over a flat plate infinite in the y-direction as shown in figure 2. Now, the known results for the laminar boundary layer can be reasoned in either of the following two ways (see ref. 5):

(a) Assume that the boundary-layer growth is determined by the length of plate that has been traversed and by the streamwise potential flow outside the boundary layer. This means that the yawed leading edge has no effect on the boundary layer and, hence, the boundary-layer thickness is given by (see ref. 6, pp. 54 and 136)

$$\delta_a = k\xi \Big/ Re_\xi^{1/2} \tag{8}$$

where

k universal constant

$Re_\xi = U_1 \xi / \nu$

(b) Assume that the geometry demands that the resultant boundary-layer growth be perpendicular to the leading edge. At each chordwise position, therefore, the spanwise potential flow is along a layer of constant thickness. Hence, it might be expected that the boundary-layer growth is determined by the chordwise flow. This leads to

$$\delta_b = kx \Big/ Re_x^{1/2} \tag{9}$$

where

$$Re_x = U_{1x} x / \nu$$

A comparison of δ_a from equation (8) and δ_b from equation (9) gives

$$\xi = x / \cos \Lambda$$

---

[1]Throughout this report the phrase "flow direction in the boundary layer" will be taken to mean the direction of the mean velocity component that is parallel to the surface.

$$Re_\xi = \frac{\frac{U_{1x}}{\cos\Lambda}\frac{x}{\cos\Lambda}}{\nu} = \frac{1}{\cos^2\Lambda} Re_x$$

Therefore,

$$\delta_a = \frac{k\frac{x}{\cos\Lambda}}{\left(Re_x/\cos^2\Lambda\right)^{1/2}} = \delta_b$$

Thus, both physical assumptions lead to the same result for the laminar boundary layer, and this result agrees with that obtained directly from the differential equations just presented.

Now, apply the same assumptions to turbulent flow, where direct calculation from the differential equations is impossible. If the empirical growth law for low Reynolds numbers (see ref. 6, p. 362), namely

$$\delta = kx/Re_x^{1/5} \tag{10}$$

is used, then, by assumption (a)

$$\delta_a = k\xi/Re_\xi^{1/5} \tag{11}$$

and by assumption (b)

$$\delta_b = kx/Re_x^{1/5} \tag{12}$$

Thus,

$$\delta_a = \frac{k\frac{x}{\cos\Lambda}}{\left(Re_x/\cos^2\Lambda\right)^{1/5}} = \delta_b \cos^{-3/5}\Lambda$$

that is, the two assumptions lead to boundary-layer thicknesses differing by a factor $\cos^{3/5}\Lambda$.

It is clear that the two arguments are based on very different assumptions, namely, in (a) yaw is assumed to have no effect and the flow goes straight back while in (b) the independence principle is assumed to be a physical principle.

If the relationship between the shearing stresses and the mean velocity derivatives is not specified, these assumptions are truly independent. In order to show this explicitly, suppose in equation (1)

$$\tau_{xz} = g(U,W, \text{ and their derivatives})$$

where $g(\ )$ indicates a functional relation; then, the independence principle is not violated. If g is known, the resultant flow direction may be calculated; but only for a restricted class of functions g will this lead to the conclusion that the flow goes straight back on a flat plate. In fact, only for the specific function g that exists for laminar flow will the conclusion be reached that the flow is straight and that the results of assumptions (a) and (b) are the same.

Since the function g is unknown for turbulent flow, clearly both the boundary-layer growth and the flow direction should be measured in a yawed-plate experiment. While neither assumption (a) nor (b) is necessarily true for the turbulent-boundary-layer case, both may conveniently be used as a basis for evaluating the experimental results.

EXPERIMENTAL EQUIPMENT AND METHODS

An unyawed plate, a 30° yawed plate, and a 45° yawed plate were used for the experiments. These are shown schematically in figures 3, 4, and 5 with appropriate details. The construction of the plates differed somewhat. The 30° yawed plate was used first and was made initially 1/2 inch thick. However, in order to get a good pressure distribution and proper two-dimensional flow (in x,y,z coordinates), it was found necessary to add stiffeners and brace the plate externally. This trouble was avoided in the unyawed and 45° yawed plates by making a box construction about 2 inches thick. The leading edges of the plates were made as shown in figure 6.

In order to make the layer develop two-dimensionally in the x-direction, a 1-inch strip of sandpaper was glued to the working surface of the plate about 3/16 inch back of the leading edge. Initially, experiments were made using a trip wire for this purpose, but the sandpaper was found to be more effective. It gave more regular thickening of the layer and its distortion effect on the velocity profile had disappeared 10 inches downstream.

The plates were installed near the beginning of the working section of the low-turbulence tunnel shown in figure 7. The tunnel, at this point, is approximately 6 feet high and 3 feet wide. The plate spanned the 6-foot dimension and had its working surface about 2 feet from the fixed tunnel wall. For the 0° and 30° plates, a 5-foot section of the

flexible tunnel wall opposite the plate was removed completely. This was done originally for ease of access and as an aid in placing the stagnation point at the leading edge of the plate on the working side without the necessity of placing obstructions downstream. In the case of the 45° plate, it was found necessary to replace the tunnel wall in order to achieve a satisfactory pressure distribution on the plate.

In order to set the pressure distribution easily, a network of static-pressure holes was incorporated in each plate (see figs. 3, 4, and 5). A system of stopcocks connecting these tubes to a manifold allowed rapid selection of each individual hole. In this way the pressure distribution could be checked very quickly. No attempt was made to calibrate these holes, but they were carefully installed and then inspected with a microscope. The large number of holes allows a check against gross error due to a defective installation.

The velocity profiles were measured by traversing a single flattened pitot tube (shown in figs. 8 and 9) through the boundary layer by means of the traversing mechanism shown unmounted in figure 10(a) and in working position in figures 10(b) and 10(c). The micrometer drive allowed positioning to 0.0005 inch. The main source of positioning error was in determining the zero position of the pitot tube. The most reliable way of accomplishing this was found to be to traverse the pitot tube toward the wall until it touched its reflection on the surface of the plate (see fig. 10(c)) and then to correct the micrometer reading by one-half the width of the tube. The reflection in the wall also proved useful for lining up the flattened pitot tube parallel to the surface.

A pitot-tube rake (fig. 11) was also used to measure velocity in the boundary layer. In general, this rake was used to check the two-dimensionality of the flow because of the ease with which it could be mounted in any desired position. On the 30° plate it was also used in two cases to measure the boundary-layer growth. The results, however, are necessarily less accurate than those obtained with the traversed pitot tube. For this reason any rake data that are plotted in the results are marked as such.

Dynamic-pressure measurements were read on a slanting tube manometer with a reading accuracy of ±0.003 inch of alcohol. Small differences of pressure were read on a micromanometer with a reading accuracy of ±0.001 inch of alcohol. The free-stream dynamic pressure was about 0.485 inch of alcohol. All of the data presented in this report were recorded at a constant value of Reynolds number per foot of 250,000 (based on the free-stream velocity). Temperature and barometric-pressure changes were compensated for by appropriate variation of the free-stream velocity.

In order to measure the flow direction in the boundary layer, the yaw head shown in figures 8 and 9 was used. This instrument was set

parallel to the wall by the reflection method mentioned previously. The adjustment is critical, especially in the region of large velocity gradient near the wall; hence, repeated measurements were performed in an effort to reduce errors.

Two methods of measurement with this yaw head were used. In the first of these, the direction of the flow was determined by recording the pressure difference (read from the two slanting tubes) as the yaw head was rotated (at a fixed distance from the wall). The total angle of rotation was about 5° and generally a straight line could be drawn through the points; from the intersection with the pressure axis, the angle at which Δp is zero could be read. This measurement was made at several stations through the boundary layer, including the free stream. The flow direction at a point in the boundary layer was then determined by the difference in the angle of zero Δp when measured at the point in question and when measured in the free stream.

The second method of measurement utilized the above procedure as a calibration. The data shown in figure 12 are those given by the "yaw-head rotation" scheme just presented. An arbitrary zero reference line (given by the centering of a carpenter's level bubble cemented to the traversing head of fig. 10(c)) was established, and the yaw-head-rotation data were plotted to this reference. It will be noted that there is considerable scatter of the "calibration data." In part, this is due to the low sensitivity of the level bubble (1/4 inch per degree, approximately) and the coarse (1°) divisions on the traversing-head protractor, as well as to the effect of a lower value of q on the sensitivity of the yaw head. In practice, the single calibration line shown in figure 12 was used; the errors in the measured flow direction are of the order of $\pm 1/3^\circ$ and this uncertainty in the angle of flow is of low order in the integrated quantity ϑ_{uv}. The yawmeter calibration was used as follows: The yaw head was set up at the 0° position and $\Delta p/q$ was read. The calibration curve gives the flow direction. Again, the reference flow direction is taken as the free stream.

EXPERIMENTAL RESULTS AND DISCUSSION

Pressure Distribution

The static pressure distribution was recorded frequently during the experiments. The results for the unyawed plate are shown in figure 13(a), for the 30° yawed plate, in figure 13(b), and for the 45° yawed plate, in figure 13(c). The differences in pressures near the leading edge indicate slightly different positions of the stagnation point, which caused no measurable differences in the velocity profiles downstream.

Since the primary purpose of this investigation was to determine the effect of yaw on the growth of the boundary layer, it seems important to consider here the possible effects of variations of pressure distribution from plate to plate (figs. 13(a) to 13(c)). The effect of these small pressure gradients may be estimated by use of the Buri form of the integrated momentum equation (see, for instance, ref. 6) as follows:

$$\vartheta_x = 0.0366\nu^{0.2}U^{-3.4}\left(\int_{x_o}^{x} U^4\,dx + C\right)^{0.8}$$

For simplicity, and since the measured pressure distributions exhibit a tendency toward periodicity, let

$$U = U_1 + U_\epsilon \sin \alpha x = U_1\left(1 + \frac{U_\epsilon}{U_1} \sin \alpha x\right)$$

where

U_1 free-stream velocity

U_ϵ amplitude of velocity variation

$\alpha = \frac{2\pi}{\lambda}$, where λ is wavelength of velocity variation

Using this value for U and noting that the value of U_ϵ/U_1 is small compared with 1, give

$$\vartheta_x = 0.0366\nu^{0.2}U_1^{-0.2}\left(1 - 3.4\,\frac{U_\epsilon}{U_1} \sin \alpha x\right)\left[x - x_o + 4\,\frac{U_\epsilon}{U_1}\left(-\frac{1}{\alpha} \cos \alpha x\right)_{x_o}^{x} + C\right]^{0.8}$$

For transition artificially fixed at the origin, $x_o = 0$, $\vartheta_o = 0$, and, hence, $C = 0$. Using these conditions, expansion of the exponential term (neglecting higher order quantities) yields

$$\vartheta_x = 0.0366\nu^{0.2}U_1^{-0.2}\left(1 - 3.4\,\frac{U_\epsilon}{U_1} \sin \alpha x\right)\left\{x^{0.8}\left[1 - \frac{3.2}{\alpha x}\,\frac{U_\epsilon}{U_1}\left(\cos \alpha x - 1\right)\right]\right\}$$

For the case of zero pressure gradient and artificially fixed transition at the origin, the Buri equation reduces to

$$\vartheta_{x_o} = 0.0366\nu^{0.2}U_1^{-0.2}x^{0.8}$$

Forming the ratio between ϑ_x and ϑ_{x_o} yields

$$\frac{\vartheta_x}{\vartheta_{x_o}} = 1 - \frac{U_\epsilon}{U_1}\left\{3.4 \sin \alpha x + \frac{3.2}{\alpha x}(\cos \alpha x - 1)\right\}$$

This relation has been evaluated for the unyawed and 45° yawed cases using wavelengths and U_ϵ determined from figures 13(a) and 13(c). The calculated change in ϑ due to the differences in the pressure distributions is less than 2 percent. This effect is therefore believed to be within the experimental accuracy of the boundary-layer measurements.

Two-Dimensionality and Flow Direction

Checks on the two-dimensionality of the flow (in x,y,z coordinates) were first made by doing spanwise traverses with the rake. As has been mentioned, stiffeners and external bracing were added to the 30° yawed plate to improve the two-dimensionality of the flow. In the course of these changes, however, only very minor effects were observed in the velocity profiles along the streamwise center line, which indicates that adequate two-dimensionality was attained. On the unyawed plate no difficulty in this respect was encountered.

The mean flow direction in the boundary layer was measured carefully on the 30° yawed plate at distances of 15.9 inches, 31.9 inches, and 47.9 inches from the leading edge in the streamwise direction. In the outer part of the layer, between $z/\delta = 0.2$ and $z/\delta = 0.1$, there was no measurable deviation from the potential flow direction. For $z/\delta < 0.2$, as the yawhead entered the steep velocity gradient near the wall, the flow-direction reading became critically dependent upon whether the flattened yawhead was exactly parallel to the wall. In this region the results are necessarily less accurate, but it was determined that the mean flow did not deviate by more than ±1° from the potential flow direction.

The flow direction in the boundary layer of the 45° plate was the subject of intensive investigation in connection with the question of possible divergence or convergence of boundary-layer flow in the test region. At the time of the completion of the growth curves, Clauser (see ref. 7) pointed out that small changes in the flow direction in the boundary layer might result in large errors in a measured growth curve. For this reason,

extensive measurements of flow-direction profiles were undertaken, and the value of the mixed momentum thickness ϑ_{uv} was determined at several stations blanketing the test region. The results of these measurements are shown in figures 14, 15, and 16. Figure 14 shows a typical flow-direction profile obtained from the calibration curve of the yawhead. In figures 15 and 16 the distributions of ϑ_{uv} over the test region are displayed.

The significance of these results is discussed in appendix A, but, for emphasis, it is noted here that congruent velocity profiles are not sufficient to assure two-dimensional flow. The angles of yaw in the boundary layer, although small enough to be undetected by pitot-tube traverses, may result in a net flow into or out of the test region which would result in important changes in the rate of growth of the boundary layer.

Velocity Profiles

The measured velocity profiles for the three flat plates are shown in figures 17(a), (b), and (c). A table of values of the displacement thickness δ^*, the momentum thickness ϑ, and the shape parameter H, computed from the velocity-profile data, is included in each of the figures. In all runs, the Reynolds number per foot (based on the free-stream velocity) was adjusted to the value of 250,000 noted in these figures.

A reduction of the velocity profiles to nondimensional form as $\frac{U}{U_1} = f\left(\frac{z}{\delta^*}\right)$ for each plate is shown in figure 18. For comparison, the nondimensional velocity profile measured on the fixed wall of the tunnel (fig. 7) is also plotted. It is seen that the effects (if any) of yaw on the velocity profile are quite small.

Virtual Origin

The experiments of Klebanoff and Diehl (ref. 3) have shown that, when sandpaper is used to promote turbulence in the boundary layer, the conditions downstream of the point where the velocity profile has returned to normal are the same as if the layer had developed from a natural transition. If a growth law is specified, this leads to the definition of a virtual origin for the boundary layer. The boundary-layer growth in these experiments is measured in terms of displacement thickness δ^* because of the difficulty in defining and measuring the actual thickness δ. The method of finding the virtual origin for the unyawed plate is as follows:

It is assumed that

$$\delta^* = \frac{k(\xi + \xi_o)}{Re^{1/5}}$$

where

k constant, 0.046

ξ distance from leading edge of plate

ξ_o distance from virtual origin to leading edge

$$Re = \frac{U_1(\xi + \xi_o)}{\nu}$$

This growth law follows the form of the empirical law mentioned previously. No claim is made that this is an exactly correct law for δ^*, but it certainly gives nearly the correct dependence on streamwise distance and Reynolds number (ref. 6, p. 362) for $Re < 3{,}000{,}000$. Hence, it is satisfactory to use this law for comparing the boundary-layer thicknesses on the yawed and unyawed plates. To determine the virtual origin (see fig. 19), the curve

$$\delta^* = \frac{kX}{Re_X^{1/5}}$$

where X is the distance from the vertical origin, is first plotted. The experimental points are fitted to this curve by shifting them along the X-axis. The position of the virtual origin is then given by $\xi_o = X - \xi$. In this way ξ_o was found to be 9 inches for the unyawed plate.

Virtual Origin for Yawed Plates

It is obviously necessary to find the virtual origin for the yawed plates by some other method, since the growth law on a yawed plate is not known but, instead, is precisely what is to be determined in the investigation. The exact effect of yaw on ξ_o is unknown, but the following limits can be established:

(1) ξ_o may depend only on the <u>streamwise</u> flow; that is, the virtual origin is 9 inches (in the streamwise direction) ahead of the leading edge.

(2) ξ_0 may depend only on the chordwise flow; that is, the virtual origin lies 9 inches (in the chordwise direction) ahead of the leading edge.

These assumptions are based on experiments regarding the effect of sandpaper for the production of turbulent boundary layers on unyawed plates. These experiments are discussed in appendix B.

The growth of the turbulent boundary layer on each of the three plates tested is shown in figure 20(a). This figure represents the raw data, as computed from the measured velocity profiles, no corrections having been made for the location of the virtual origin. As before, the Reynolds number per foot (based on free-stream velocity) was kept constant at 250,000.

If the above assumptions regarding the virtual origin are applied to the data, figures 20 and 21 are obtained. Figure 20(a) (with the abscissa shifted 9 inches) represents assumption (1), while figure 20(b) gives the result of assumption (2). Figures 21(a) and 21(b) are logarithmic plots of the same data as are given in figures 20(a) and (b), respectively. In each of these figures, two curves marked "Independence principle" have been drawn. These curves represent the data from the unyawed plate plotted against the appropriate streamwise coordinate ($\xi = x/\cos \Lambda$) for the two cases $\Lambda = 30^\circ$ and $\Lambda = 45^\circ$. It is evident, as far as the applicability of the independence principle is concerned, that the difference in the virtual origins given by assumptions (1) and (2) is of no consequence.

Boundary-Layer Growth

The conclusion at this point is unmistakable: The independence principle cannot be applied to the case of turbulent boundary layers on yawed flat plates. The measured growth curve, for the cases $\Lambda = 30^\circ$ and 45° is thicker than that for the unyawed-plate case, while the independence principle predicts a thinning effect of yaw.

The logarithmic plot of figure 21(a) is of special interest. Note that a virtual origin of 9 inches for each case has been assumed; straight lines with slope equal to 4/5 have been drawn through the experimental data. The values of the constant C (see fig. 21(a)) for these straight lines for the three angles of yaw have been noted in the figure. They are very nearly in the same ratio as $\cos^{2/5}\Lambda$. From a purely empirical standpoint, then, the curve of figure 22(a) may be drawn. Note that the data are reduced to a single curve by the inclusion of the empirical $\cos^{2/5}\Lambda$ factor. This is shown also in the Cartesian plot of figure 22(b).

The empirically determined growth law is given by

$$\delta^* = \frac{0.046}{\cos^{2/5}\Lambda} \frac{\xi_o + \xi}{Re_\xi^{1/5}}$$

The growth law which is given by the assumption of the independence principle is

$$\delta^* = 0.046 \cos^{3/5}\Lambda \frac{\xi_o + \xi}{Re_\xi^{1/5}}$$

where in each of the above expressions

$$Re_\xi = U_1\left(\xi_o + \xi\right)/\nu$$

Thus, the two growth curves differ by a factor equal to $\cos \Lambda$. In the case of the plate yawed 45° this represents a large difference, more than can be explained on the basis of any known experimental inaccuracy.

It must be emphasized, however, that the empirical growth law noted above is the result of only three experiments and thus should be considered as merely a tentative result until more extensive experimental confirmation is available.

Results of Young and Booth

Prior to the present investigation, the only experimental data available regarding the turbulent boundary layer on yawed flat plates were those obtained by Young and Booth (ref. 4). In their experiments, which were stated to be preliminary, a single plate, with a boundary-layer trip wire, was rotated to angles of yaw of 20°, 30°, and 45° and the boundary-layer thickness at a single chordwise station, as well as the total drag of plate and wire, was measured. The principle results of their investigation may be stated as follows:

(a) The independence principle does apply.

(b) The flow in the boundary layer is in the direction of the free stream.

The results of the present investigation are in direct contradiction to the first of the Young and Booth results. Since Young and Booth have not presented the complete details of their experiment, it is difficult to assess the exact source of the discrepancy. The present authors feel

that a likely origin of error in any boundary-layer investigation of this nature is departure from two-dimensionality of the flow. As pointed out previously, the presence of divergence or convergence of the flow in the boundary layer can have important consequences on boundary-layer-thickness measurements.

Another possible source of error is the effect of yaw on the action of a trip wire in causing transition. The wire presumably lies in an area of laminar flow; hence, its significant Reynolds number varies as $\cos \Lambda$ in the experiments. It is known that transition does not occur at a trip wire but some distance downstream. The influence of a considerable variation of Reynolds number on this distance, and therefore on the virtual origin of the turbulent layer, is not known. Although this effect was found in the present investigation (appendix B) to be negligible for sandpaper transition strips, the same may not be true for a trip wire.

CONCLUDING REMARKS

The results of measurements in the turbulent boundary layer on three flat plates yawed 0°, 30°, and 45° indicate that the boundary-layer displacement thickness increases in the stream direction at a slightly greater rate on the yawed plates than it does on the unyawed plate.

An empirical growth law, including this effect of yaw, has been determined. It is emphasized that this law may apply only to the experimental setup described.

The effects of yaw on the direction of flow within the boundary layer have been measured. These effects are, in general, small.

Cornell University,
Ithaca, N. Y., March 22, 1954.

APPENDIX A

EFFECT OF FLOW DIVERGENCE ON MEASURED BOUNDARY-LAYER GROWTH

The incompressible-flow boundary-layer momentum equation in the direction of the x-axis is given by (see, for instance, ref. 8)

$$\frac{\partial}{\partial x}\int_0^\delta U^2 dz - U_1 \frac{\partial}{\partial x}\int_0^\delta U\, dz + \frac{\partial}{\partial y}\int_0^\delta UV\, dz - U_1 \frac{\partial}{\partial y}\int_0^\delta V\, dz = -\frac{\delta}{\rho}\frac{\partial p}{\partial x} - \frac{\tau_o}{\rho}$$

Transforming this equation to momentum-thickness terms and assuming a flat plate (zero pressure gradient) give

$$\frac{\partial \vartheta_{uu}}{\partial x} + \frac{\partial \vartheta_{uv}}{\partial y} = \frac{\tau_o}{\rho U_1^2}$$

Note that this equation is the same as that normally used to determine the wall shear with the addition of mixed-momentum-thickness terms.

In order to ascertain the effect of the non-two-dimensionality of the flow (represented by figs. 15 and 16), the derivatives in the above equation can be evaluated from the experimental data. This is most easily accomplished by recourse to the skewed ξ,ϵ coordinate system shown in figure 26. In this coordinate system,

$$\xi = x - y \tan \Lambda$$

$$\epsilon = y/\cos \Lambda$$

Hence,

$$\frac{\partial}{\partial x} = \frac{\partial}{\partial \xi}$$

$$\frac{\partial}{\partial y} = \frac{1}{\cos \Lambda}\frac{\partial}{\partial \epsilon} - \tan \Lambda \frac{\partial}{\partial \xi}$$

The equation for the x-momentum in the new coordinate system is then

$$\frac{\partial \vartheta_{uu}}{\partial \xi} + \frac{1}{\cos \Lambda}\frac{\partial \vartheta_{uv}}{\partial \epsilon} - \tan \Lambda \frac{\partial \vartheta_{uv}}{\partial \xi} = \frac{\tau_o}{\rho U_1^2}$$

The terms on the left-hand side of the equation were evaluated at $\xi = 36$ inches and $\epsilon = 14.85$ inches which represents the center of the presumed two-dimensional test region. The results are presented as follows:

$$\frac{\partial \vartheta_{uu}}{\partial \xi} = 2.09 \times 10^{-3} \qquad \frac{\partial \vartheta_{uv}}{\partial \epsilon} = -3.75 \times 10^{-5} \qquad \frac{\partial \vartheta_{uv}}{\partial \xi} = 1.85 \times 10^{-5}$$

Inserting these values into the equation for the x-momentum, and noting that $\Lambda = 45^{\circ}$, shows that the error involved in neglecting the mixed-momentum-thickness term is approximately 3 percent.

Although the correction in this case is small, it must be stated that large errors can be the result of apparently small changes in flow direction, since the value of the derivative can become quite large. In an experiment where boundary-layer growth curves are measured, it is easy to see that changes in the flow direction within the boundary layer can give erroneous results by adding air to or exhausting it from the test region. It is felt that the calculation just described indicates that the measured boundary-layer growth curves reported herein are substantially correct.

APPENDIX B

THE EFFECT OF YAW AND ROUGHNESS ON VIRTUAL ORIGIN AND TRANSITION OF AN ARTIFICIALLY THICKENED BOUNDARY LAYER

Effect of Yaw on Virtual Origin of Artificially Thickened Boundary Layer

Before any conclusions could be drawn regarding the effect of yaw on the turbulent boundary layer itself, it was necessary to consider the effect of yaw on the sandpaper used to thicken the boundary layer. While a complete experimental analysis of the situation was beyond the scope of the present investigation, several simple experiments were performed which served as a basis for the assumptions in the body of this report. These assumptions depend on the following limiting cases:

(1) Assume that ξ_o depends upon the streamwise flow. For the yawed plate, then, ξ_o is determined by $U_1/\nu = 250{,}000$ and a sandpaper width of $1 \text{ in.}/\cos \Lambda$ and should be taken in the streamwise direction.

(2) Assume that ξ_o is determined by the chordwise flow. For the yawed plate, then, ξ_o is determined by $U_1/\nu = 250{,}000 \cos \Lambda$ and by a sandpaper width of 1 inch and should be taken in the chordwise direction.

Experiments were carried out on the unyawed plate to determine how ξ_o depended upon sandpaper width and upon U_1/ν. Figure 23 shows that doubling the width of sandpaper at $U_1/\nu = 250{,}000$ had a relatively small effect in thickening the boundary layer. For a 14-percent increase in sandpaper width, as in assumption (1), then, it can be said that ξ_o would be unchanged within experimental accuracy limits. Figure 24 shows the results of varying U_1/ν for a constant sandpaper width of 1 inch. The curves are plotted assuming that ξ_o was unchanged from the value given in figure 19. The experimental points lie very close to these curves except for the lowest value of U_1/ν. It seems safe to assume, then, that for $U_1/\nu = 177{,}000 \left(= (U_1/\nu) \cos 45^\circ, \text{ the lowest possible value}\right)$ ξ_o is still 9 inches. With this evidence, therefore, the assumptions of a virtual origin for the yawed plate are, as stated previously, (1) the virtual origin is 9 inches in the streamwise direction ahead of the leading edge, or (2) the virtual origin is 9 inches in the chordwise direction ahead of the leading edge.

Use of Sandpaper to Produce Artificial Transition

In experimenting with turbulent boundary layers it is frequently necessary to use some method of artificially inducing transition from laminar to turbulent flow. The purpose may be to thicken the boundary layer, as in reference 3, or to make transition occur along a given line, as in the present investigation and in reference 4. For either of these purposes sandpaper roughening has the particular advantage that the boundary layer returns to normal in a relatively short distance downstream (ref. 3).

Figure 25 shows a determination of the virtual origins for results given in reference 3 where a strip of sandpaper 24 inches wide was used. Because of the different range of Re_x it was necessary to use a different boundary-layer growth law from that used in the present report (fig. 14). The growth law used is derived directly from the Kármán-Schoenherr formula

$$\frac{1}{C_f^{1/2}} = 4.13 \log\left(Re_x C_f\right)$$

by observing that, for a flat plate,

$$C_f = 2\vartheta/x$$

and, hence,

$$x^{1/2} = 5.85\vartheta^{1/2} \log\left(2Re_\vartheta\right)$$

A quantitative comparison of these results with the results obtained in the present investigation is difficult, but the following observations may be of interest:

For the 24-inch strip of sandpaper,

(1) The boundary layer returned to normal 66 inches downstream of the trailing edge of the sandpaper.

(2) The layer was "overthickened" immediately behind the sandpaper and hence approached the normal growth curve from above.

(3) As the free-stream velocity was increased, the virtual-origin distance increased.

For the 1-inch strip of sandpaper,

(1) The boundary layer returned to normal 10 inches downstream of the trailing edge of the sandpaper.

(2) The layer thickened more rapidly than normal immediately behind the sandpaper and approached the normal growth curve from below.

(3) For a similar increase in free-stream velocity the virtual origin did not shift proportionately as much as for the 24-inch strip of sandpaper.

REFERENCES

1. Sears, W. R.: The Boundary Layer of Yawed Cylinders. Jour. Aero. Sci., vol. 15, no. 1, Jan. 1948, pp. 49-52.

2. Jones, Robert T.: Effects of Sweepback on Boundary Layer and Separation. NACA Rep. 884, 1949. (Supersedes NACA TN 1402.)

3. Klebanoff, P. S., and Diehl, Z. W.: Some Features of Artificially Thickened Fully Developed Turbulent Boundary Layers With Zero Pressure Gradient. NACA Rep. 1110, 1952. (Supersedes NACA TN 2475.)

4. Young, A. D., and Booth, T. B.: The Profile Drag of Yawed Wings of Infinite Span. Rep. 38, College of Aero. (Cranfield), May 1950.

5. Rott, Nicholas, and Crabtree, L. F.: Simplified Laminar Boundary-Layer Calculations for Bodies of Revolution and for Yawed Wings. Jour. Aero. Sci., vol. 19, no. 8, Aug. 1952, pp. 553-565.

6. Fluid Motion Panel of the Aeronautical Research Committee and Others (S. Goldstein, ed.): Modern Developments in Fluid Dynamics. Vols. I and II. The Clarendon Press (Oxford), 1938.

7. Clauser, Francis H.: Turbulent Boundary Layers in Adverse Pressure Gradients. Jour. Aero. Sci., vol. 21, no. 2, Feb. 1954, pp. 91-108.

8. Tetervin, Neal: Boundary-Layer Momentum Equations for Three-Dimensional Flow. NACA TN 1479, 1947.

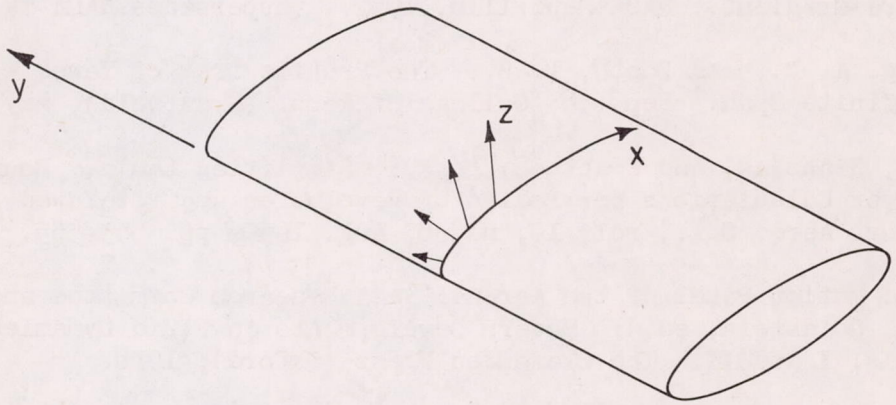

Figure 1.- Coordinate system for yawed boundary layer.

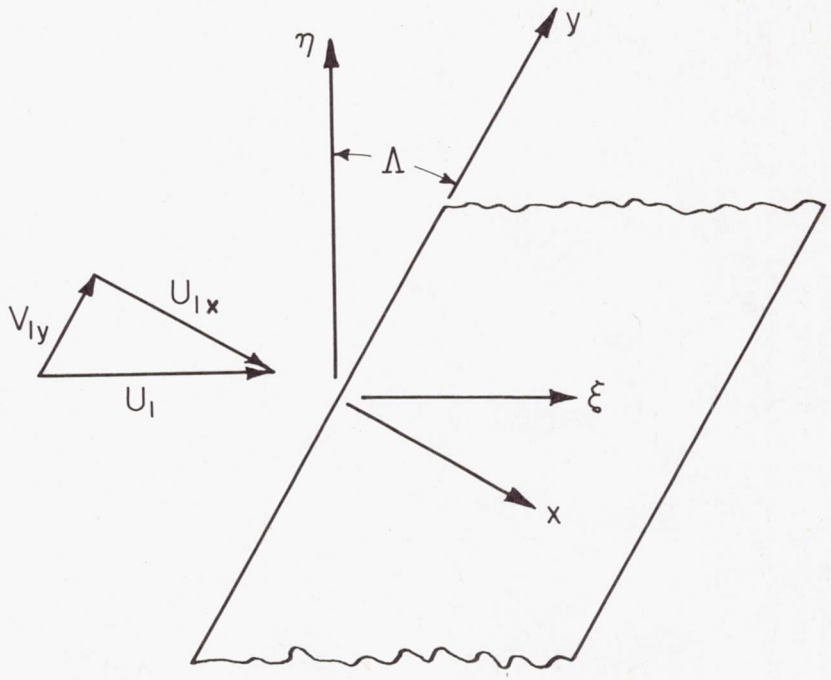

Figure 2.- Coordinate system for yawed plates.

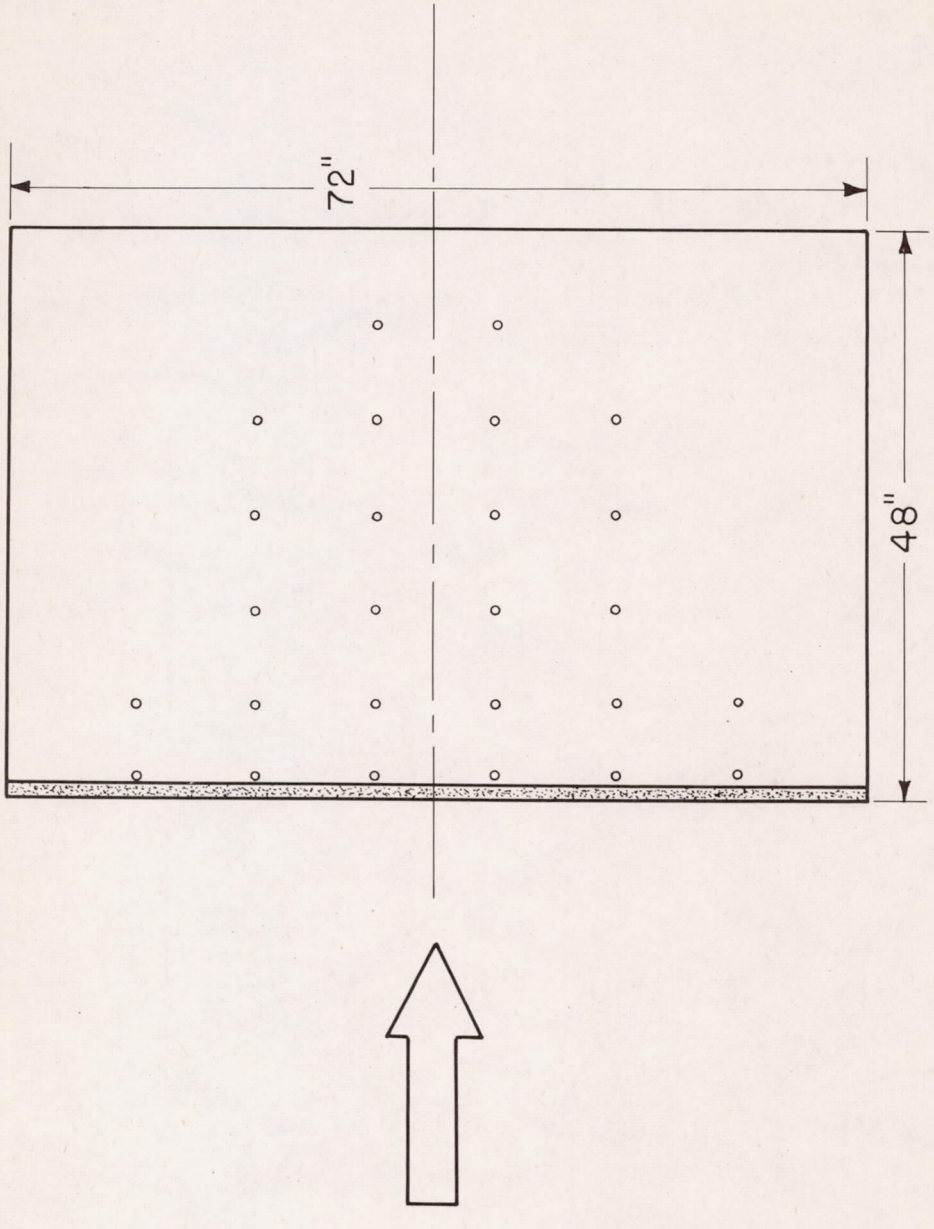

Figure 3.- Unyawed flat plate. $\frac{1}{16}$ full size.

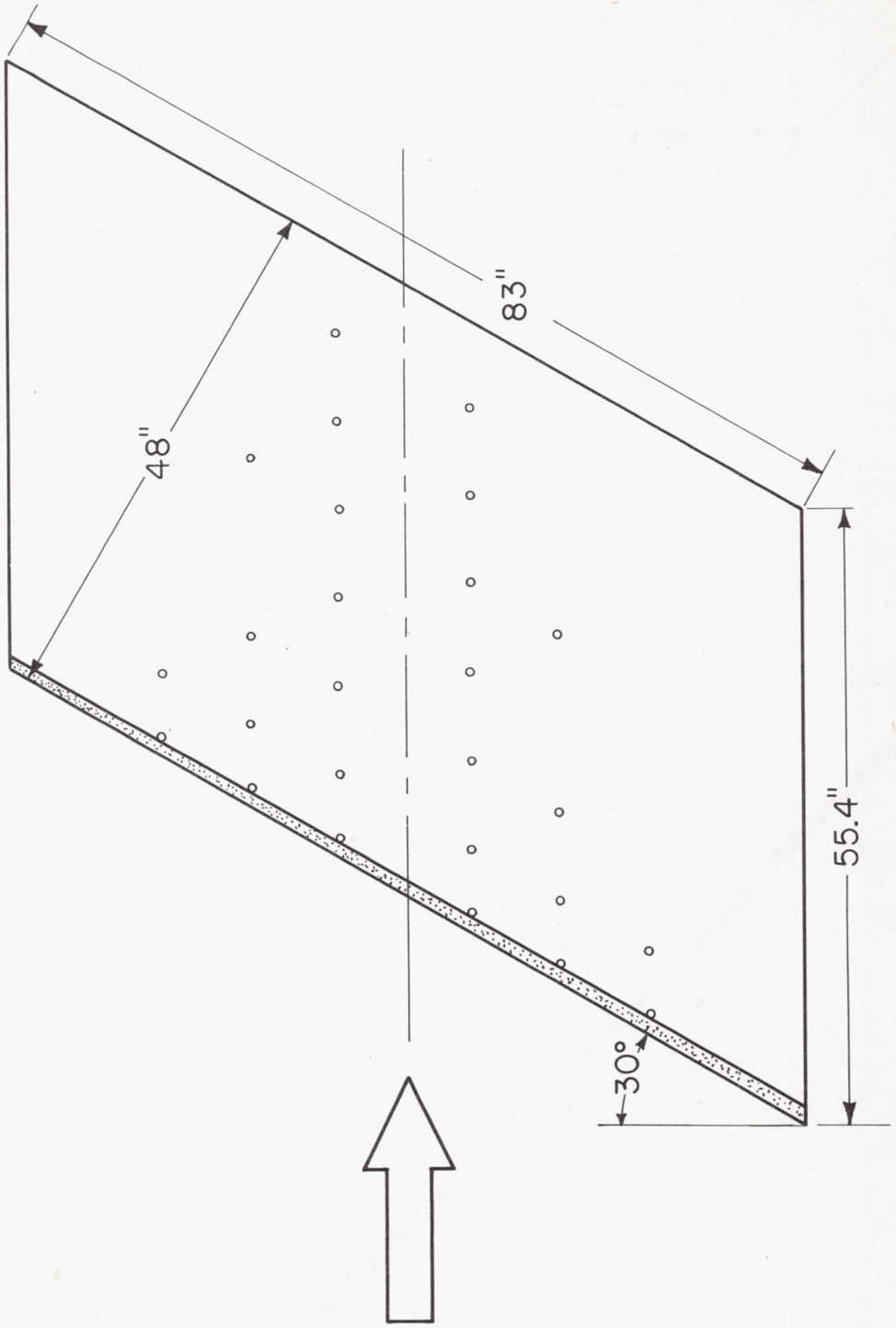

Figure 4.- Yawed flat plate. $\frac{1}{16}$ full size.

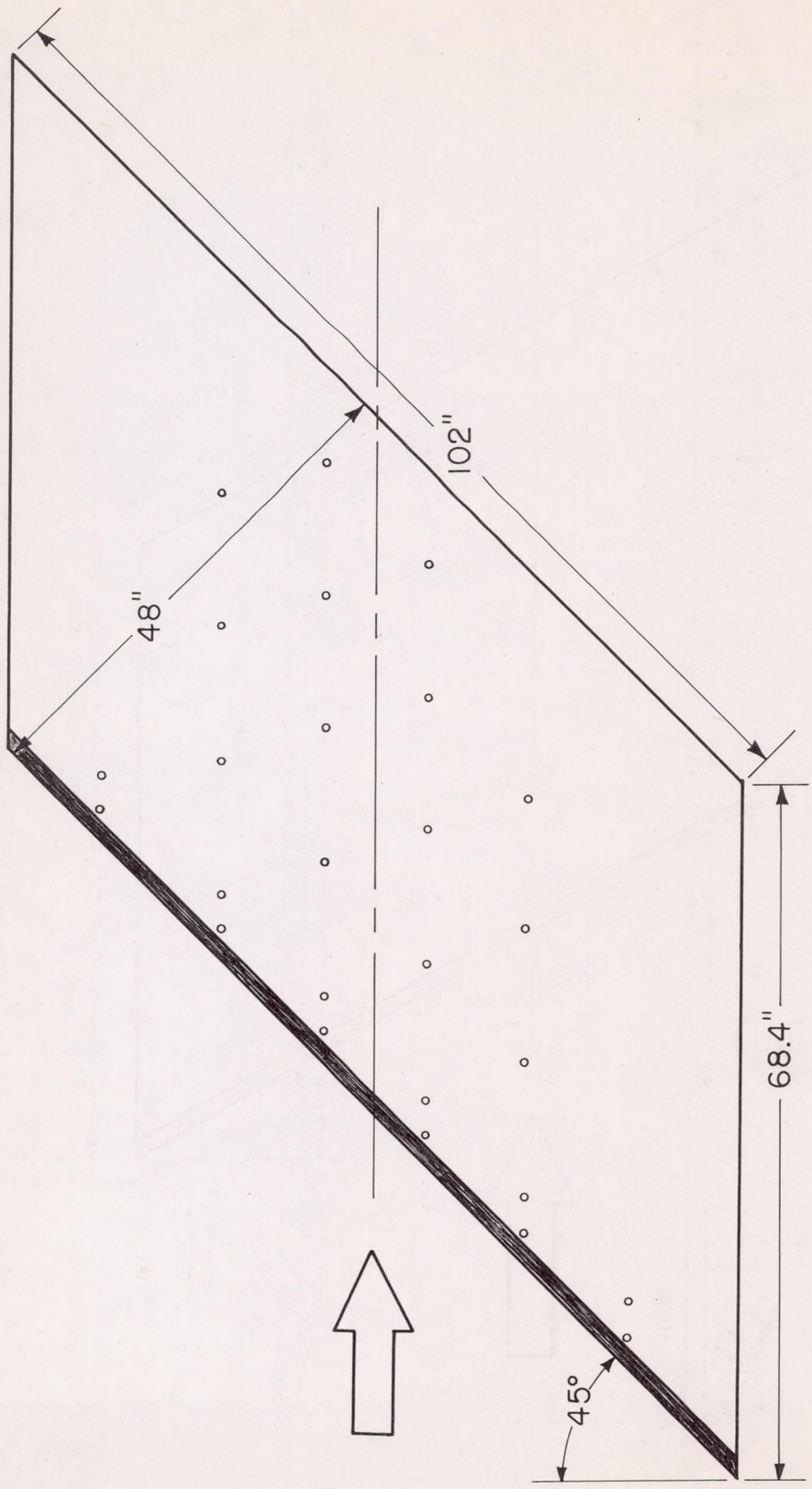

Figure 5.- 45° yawed flat plate. $\frac{1}{16}$ full size.

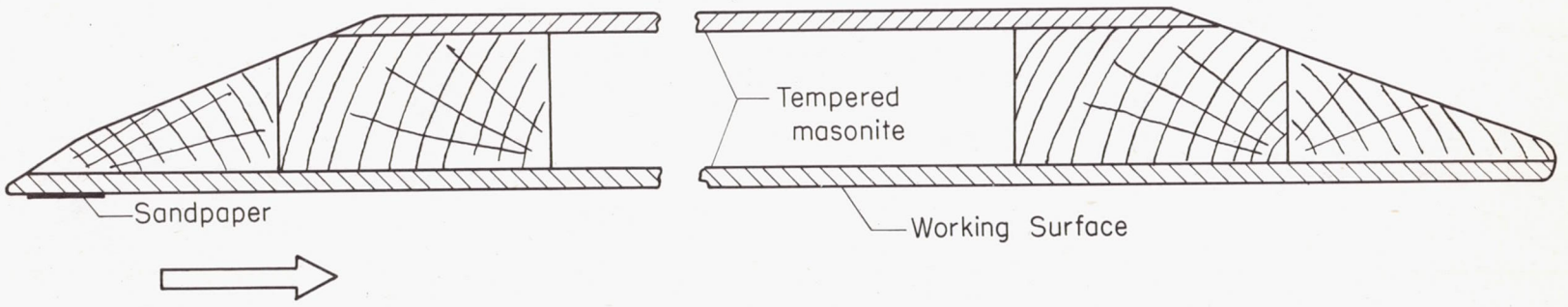

Unyawed flat plate, 45° yawed flat plate

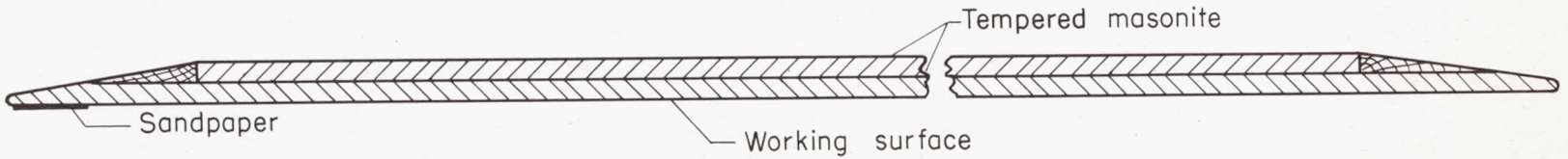

30° Yawed flat plate

Figure 6.- Plate cross sections. $\frac{1}{12}$ full size.

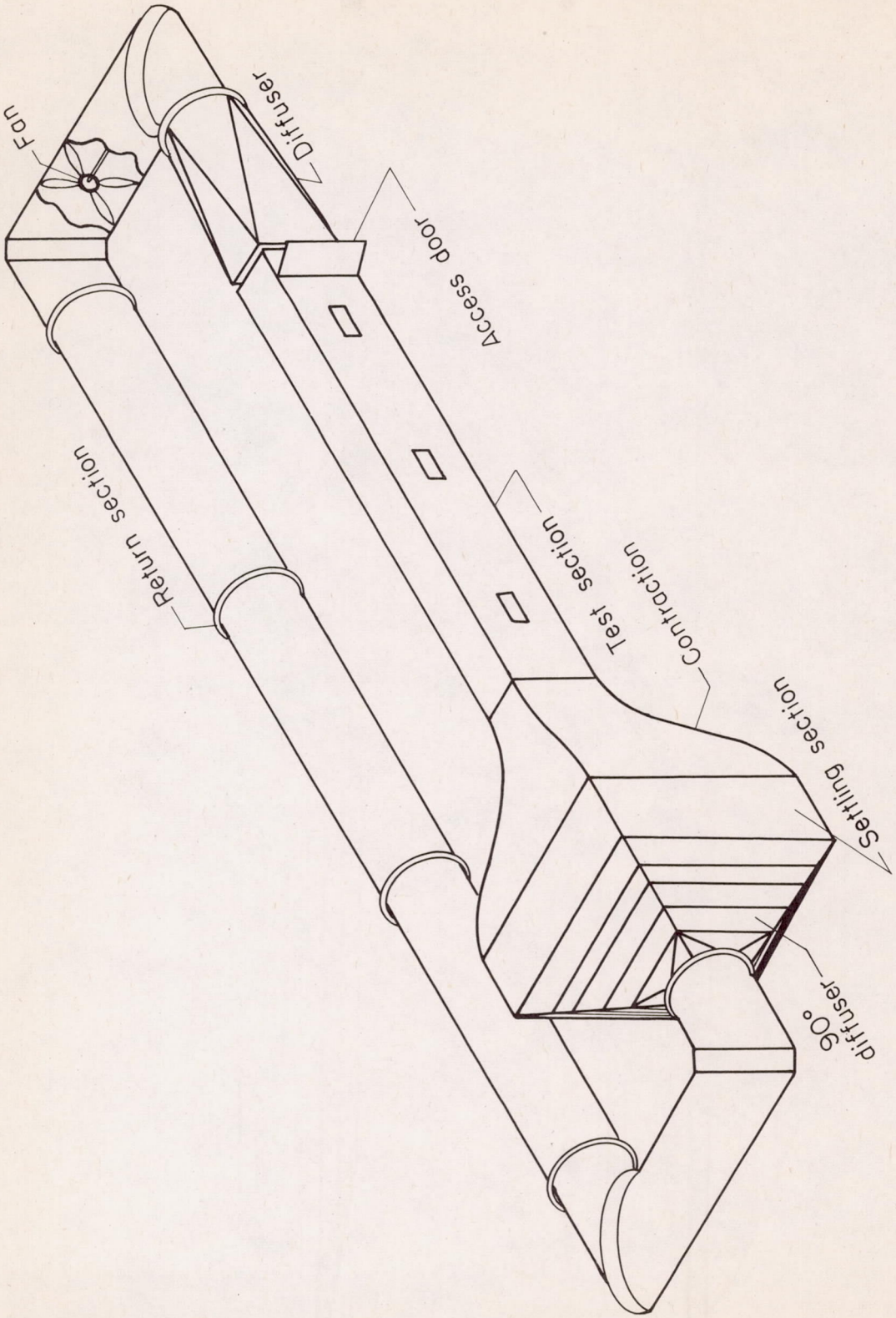

Figure 7.- Boundary-layer wind tunnel. $\frac{1}{128}$ full size.

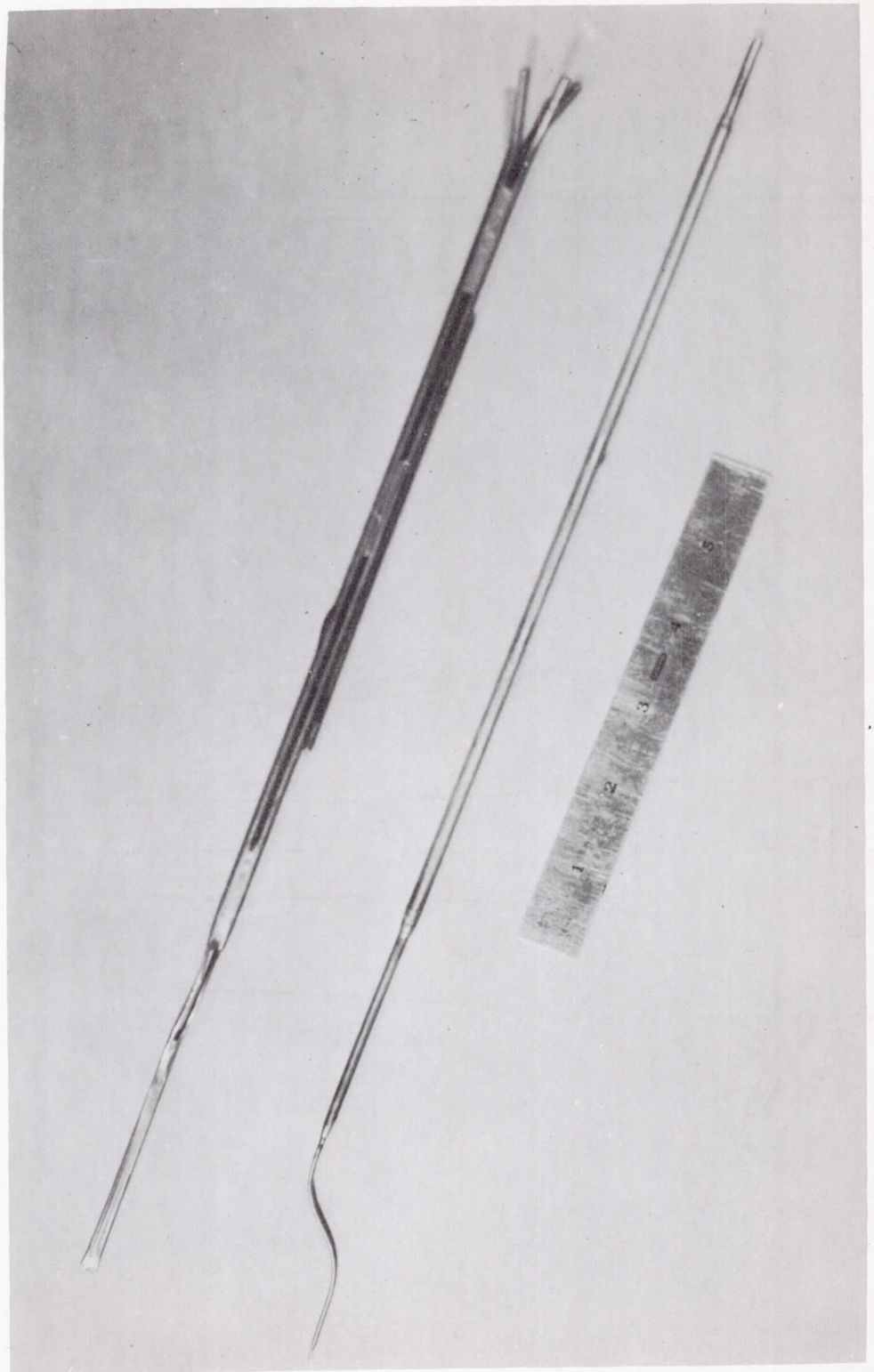

L-86492

Figure 8.- Pitot tube and yawhead.

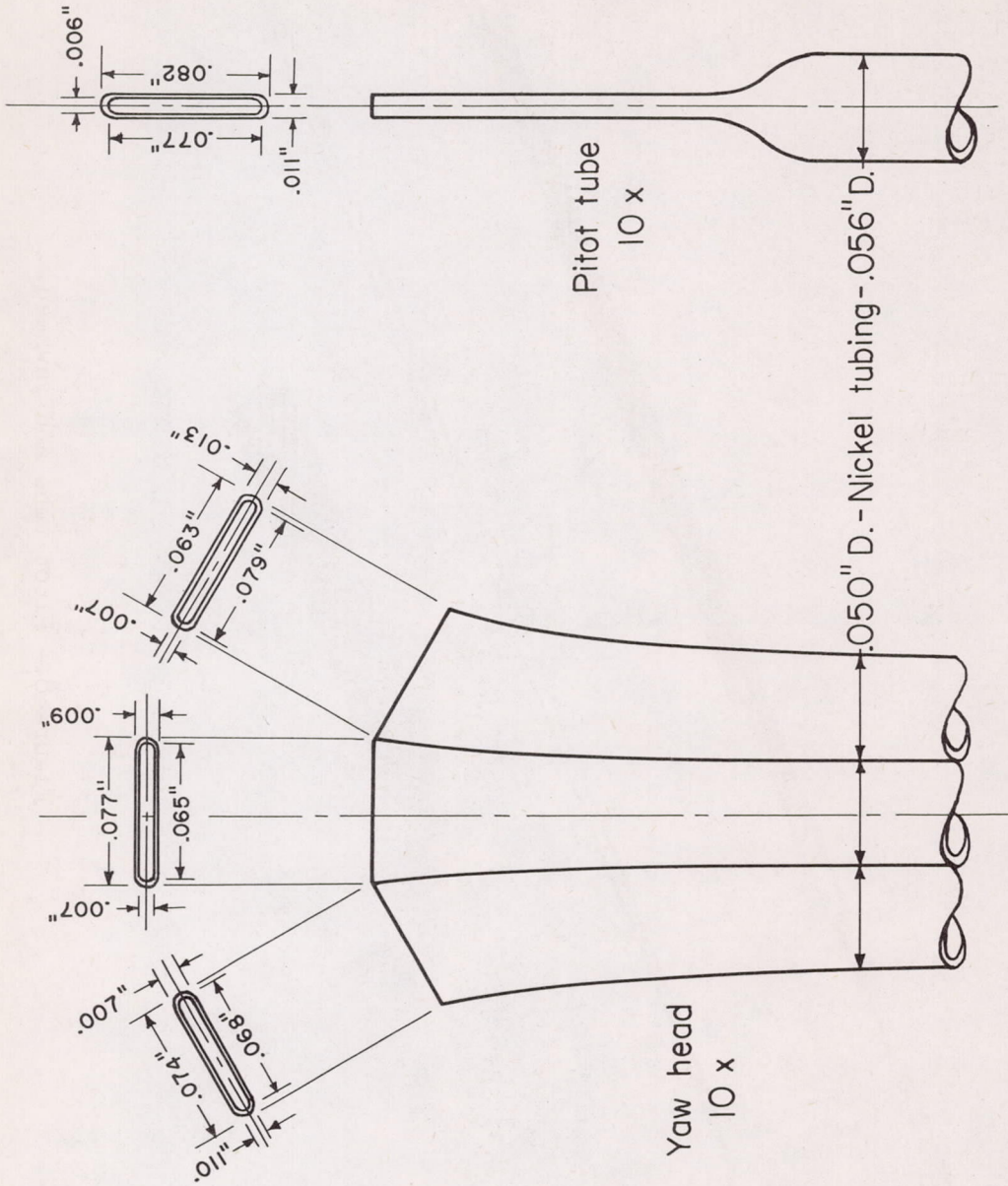

Figure 9.- Probe details.

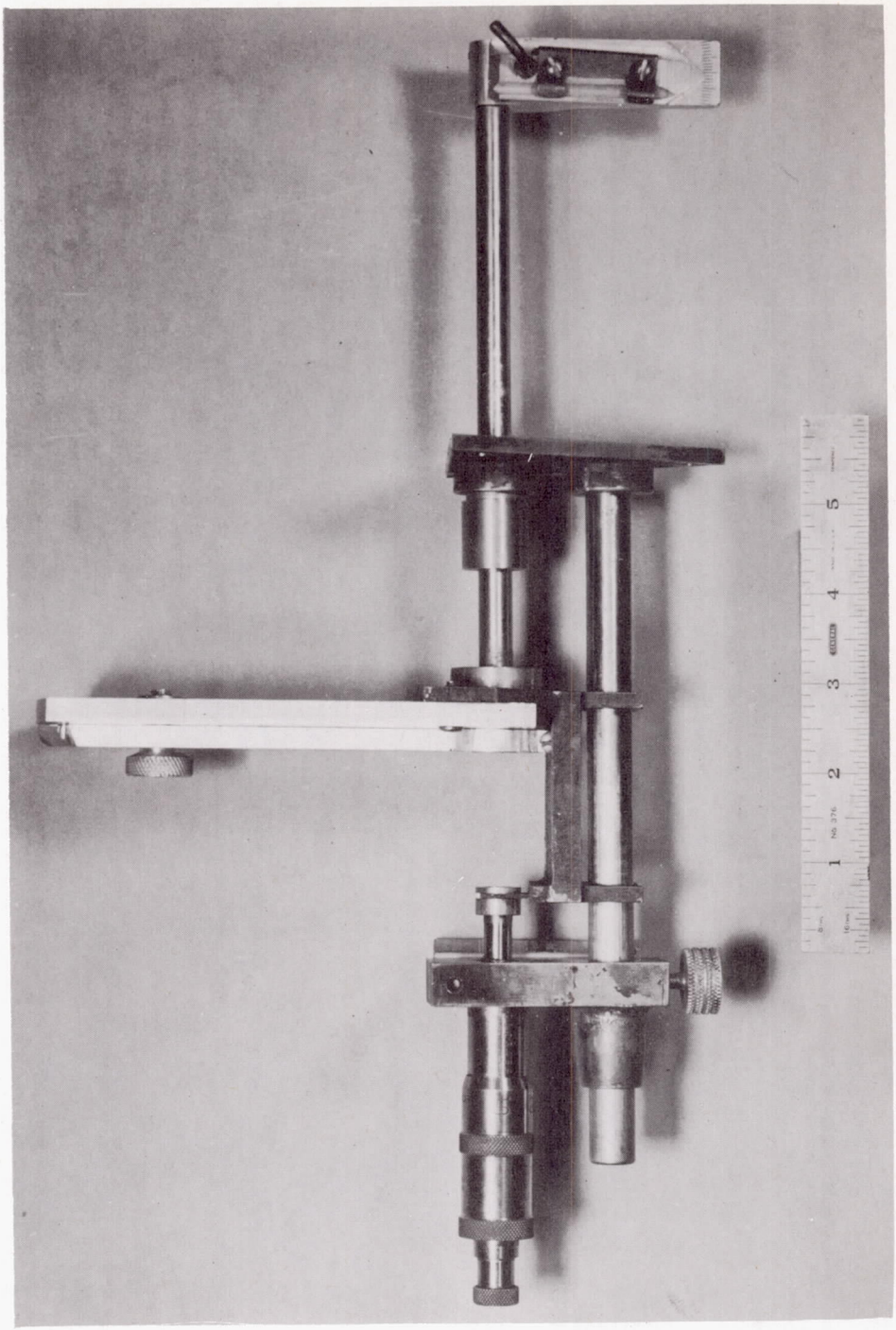

L-86493

(a) Unmounted.

Figure 10.- Traversing mechanism.

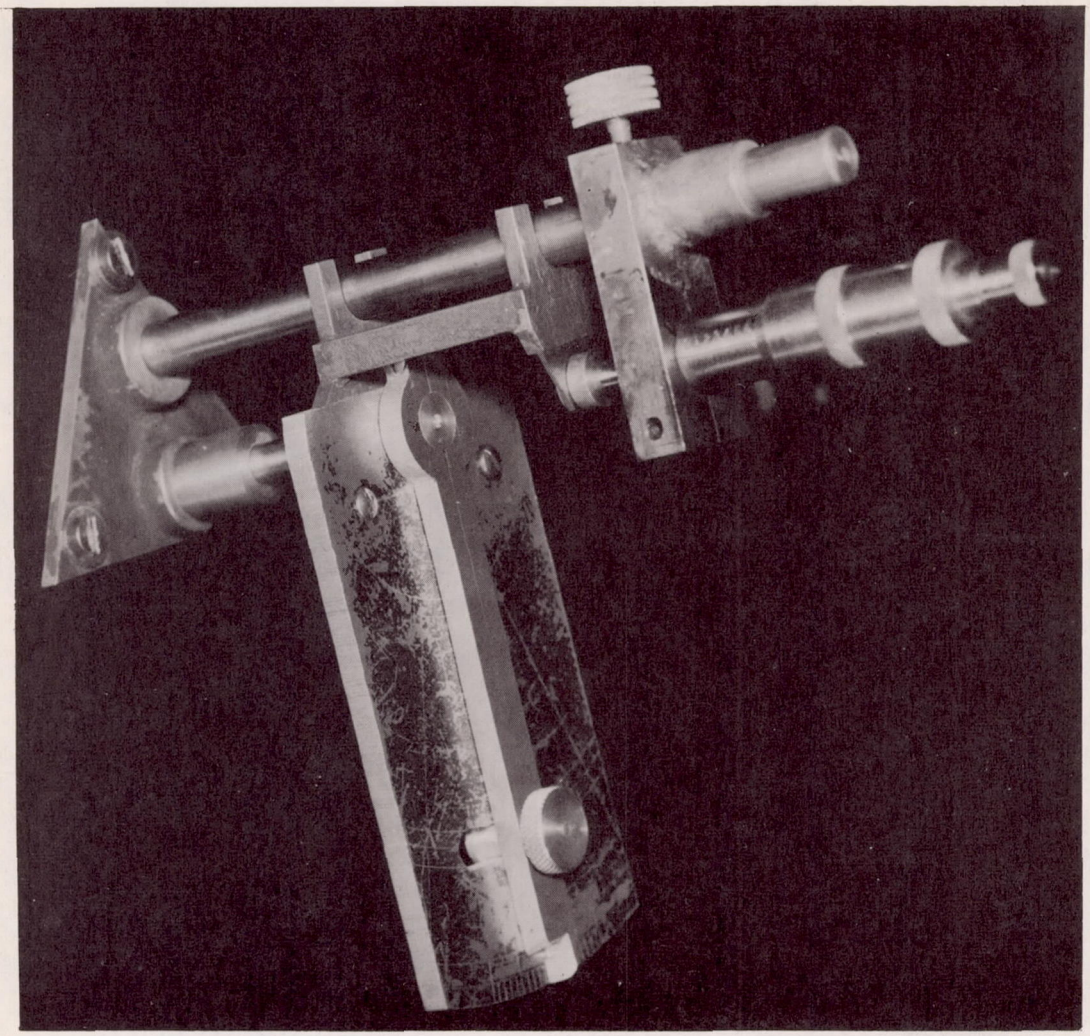

L-86494

(b) Mounted; view from back of plate.

Figure 10.- Continued.

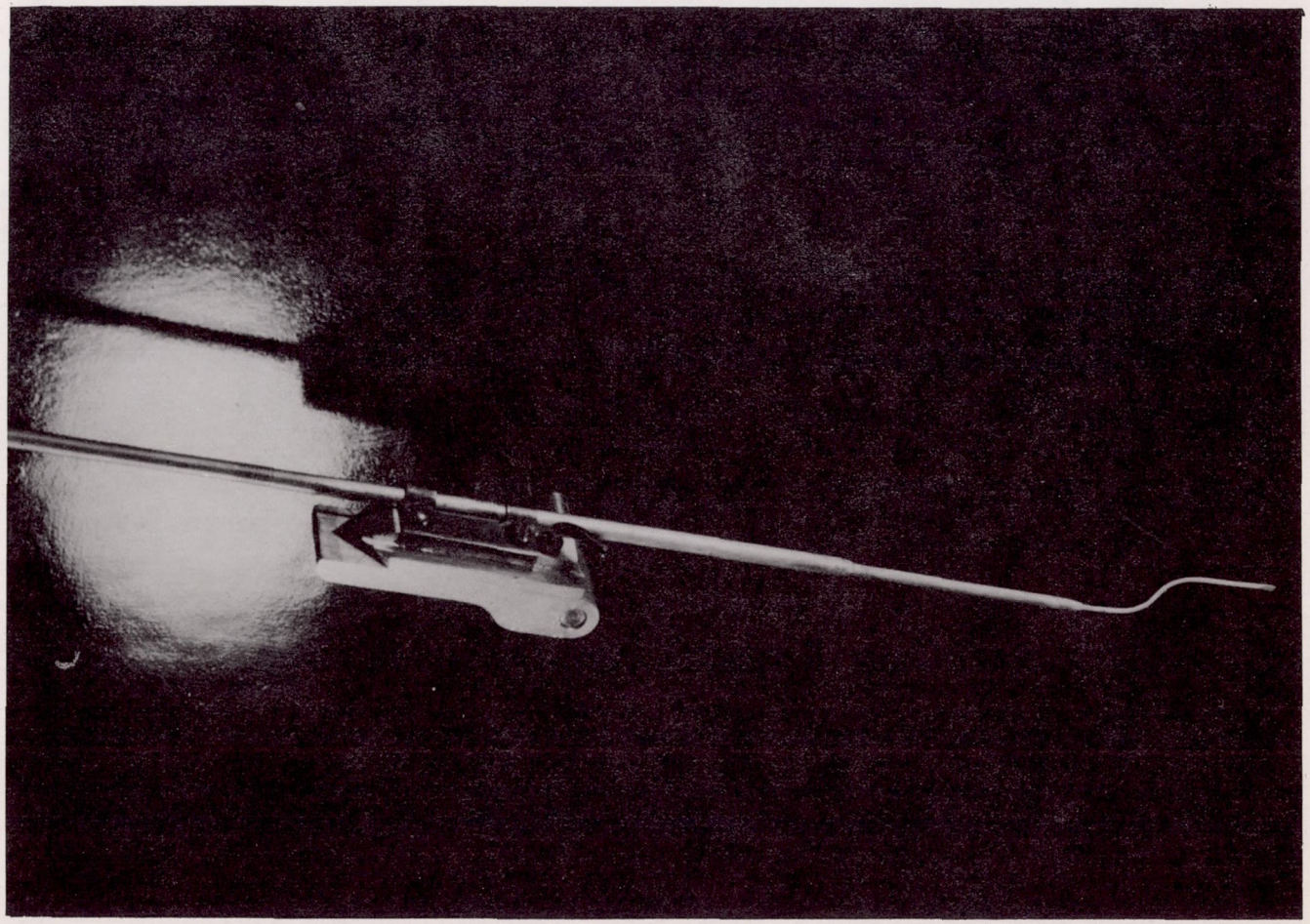

L-86495

(c) Mounted; view from working side of plate.

Figure 10.- Concluded.

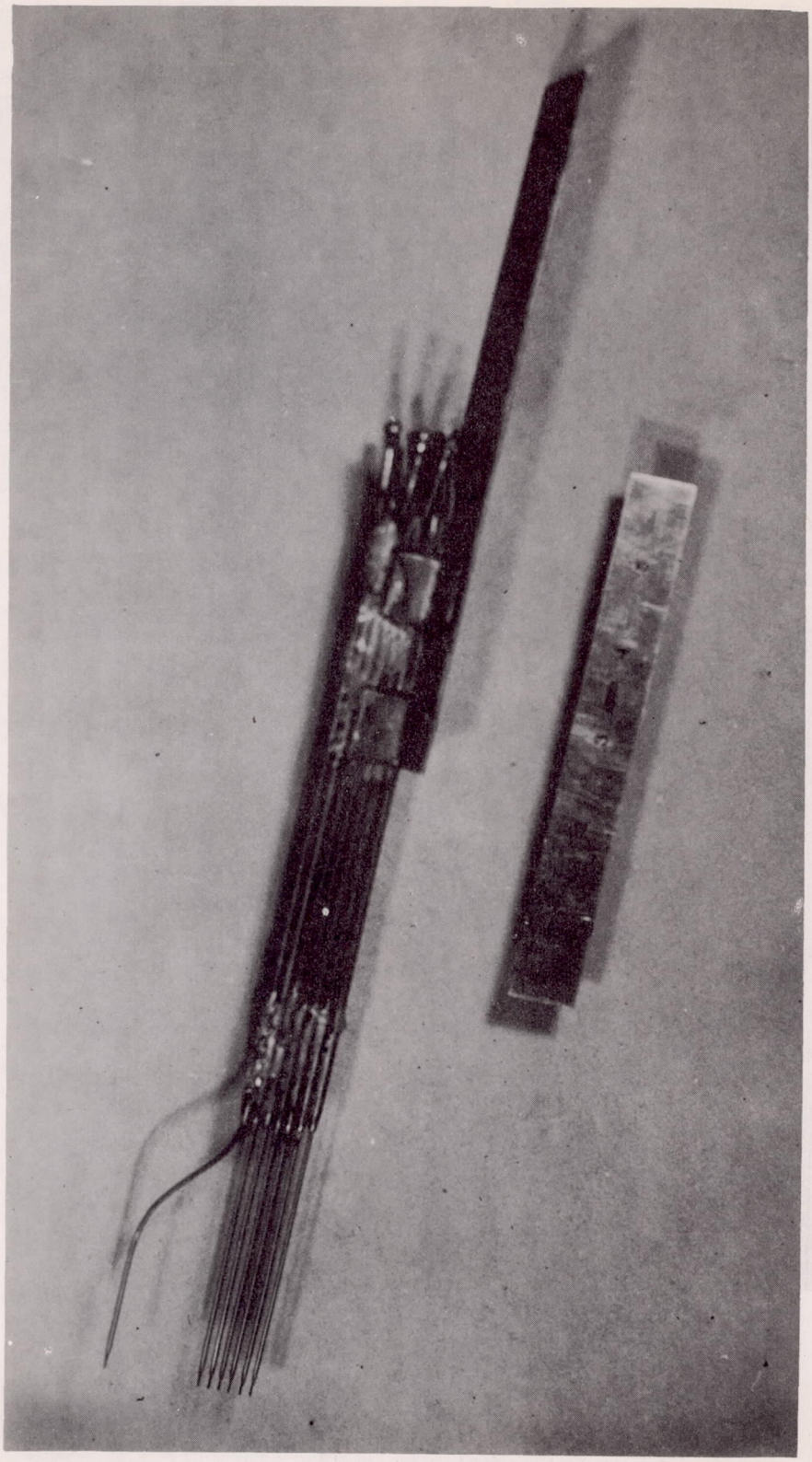

L-86496

Figure 11.- Pitot tube rake.

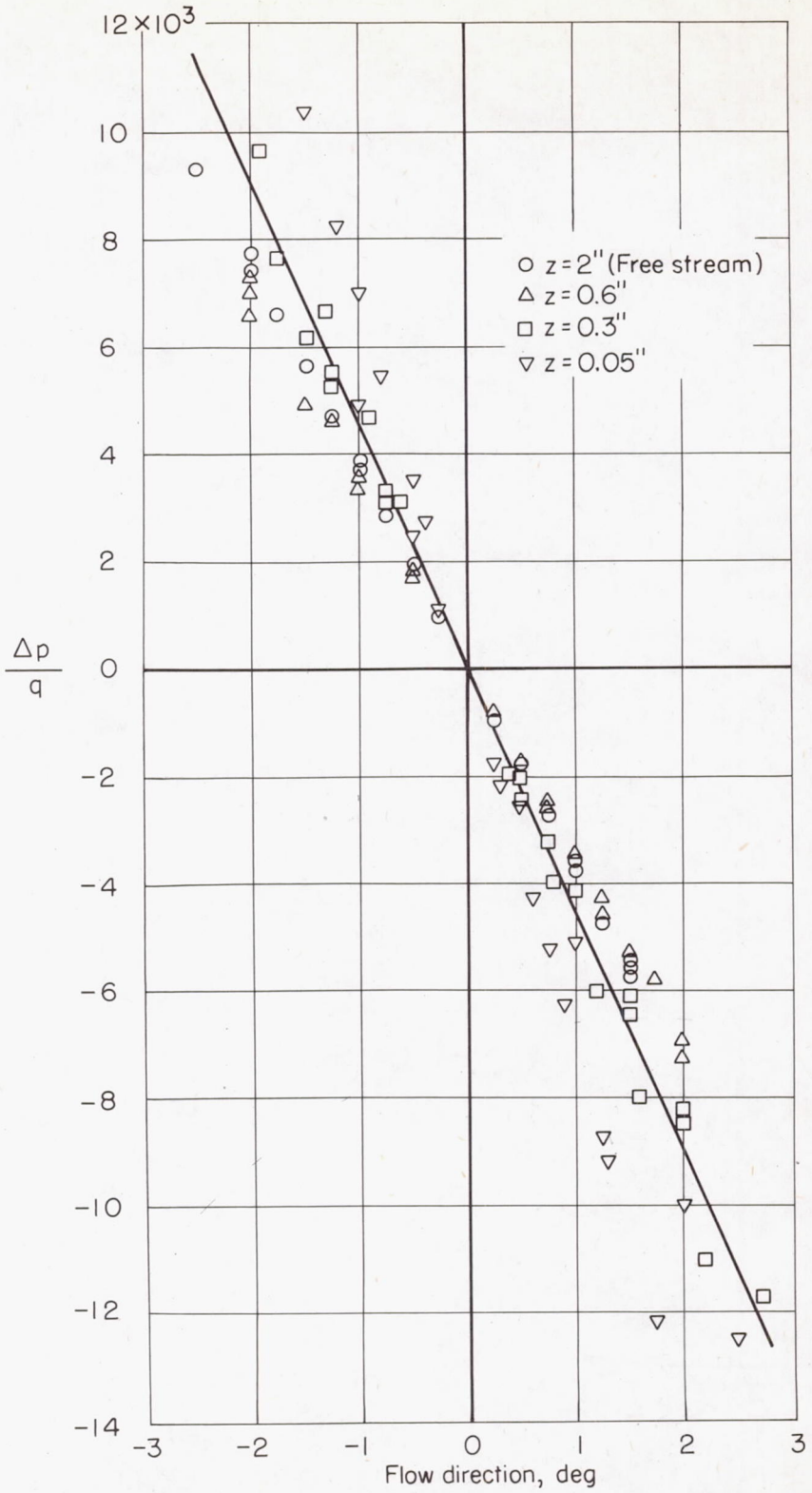

Figure 12.- Yawmeter calibration.

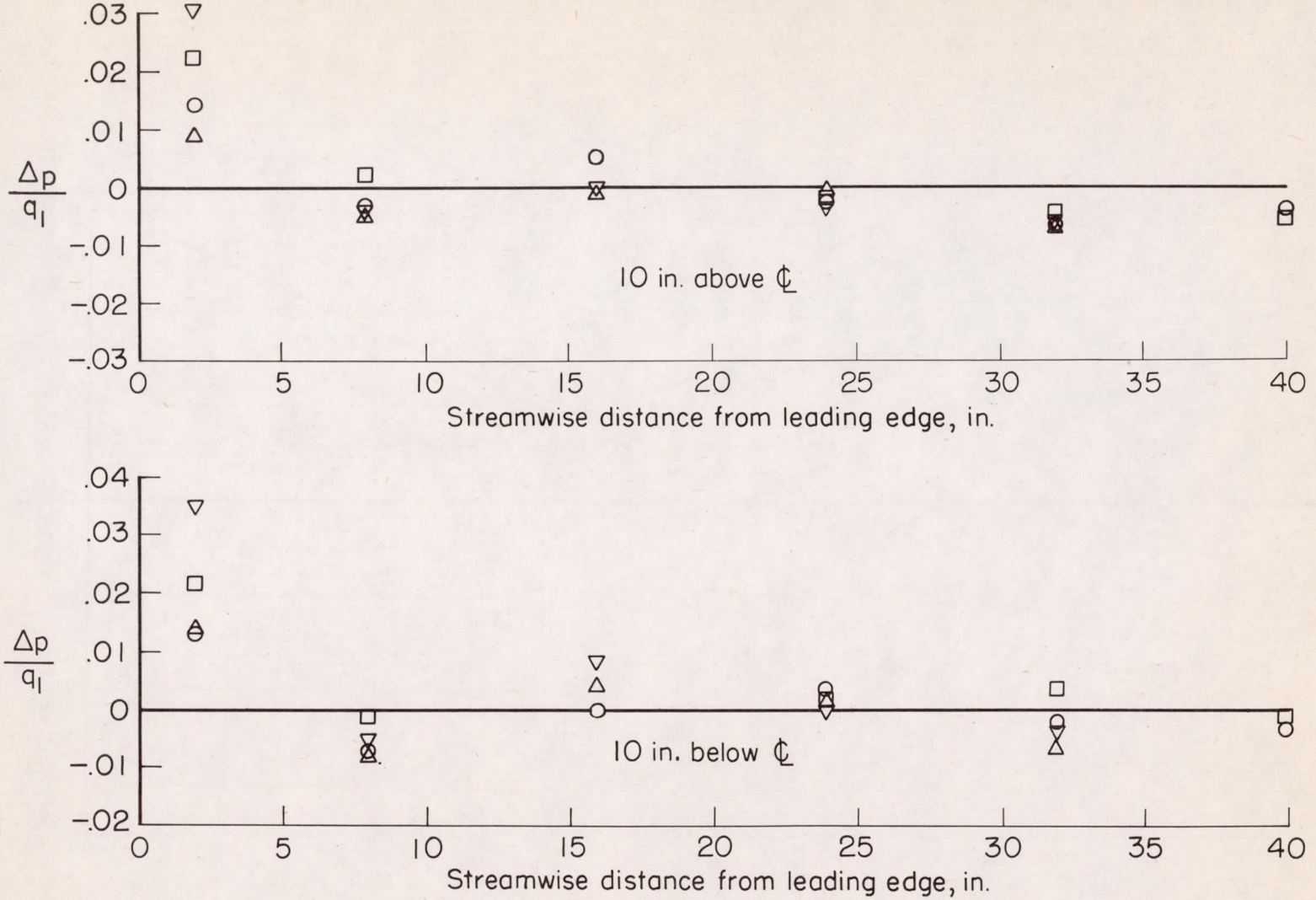

(a) Unyawed flat plate.

Figure 13.- Pressure distribution. Symbols refer to pressure-distribution check runs during course of boundary-layer measurements.

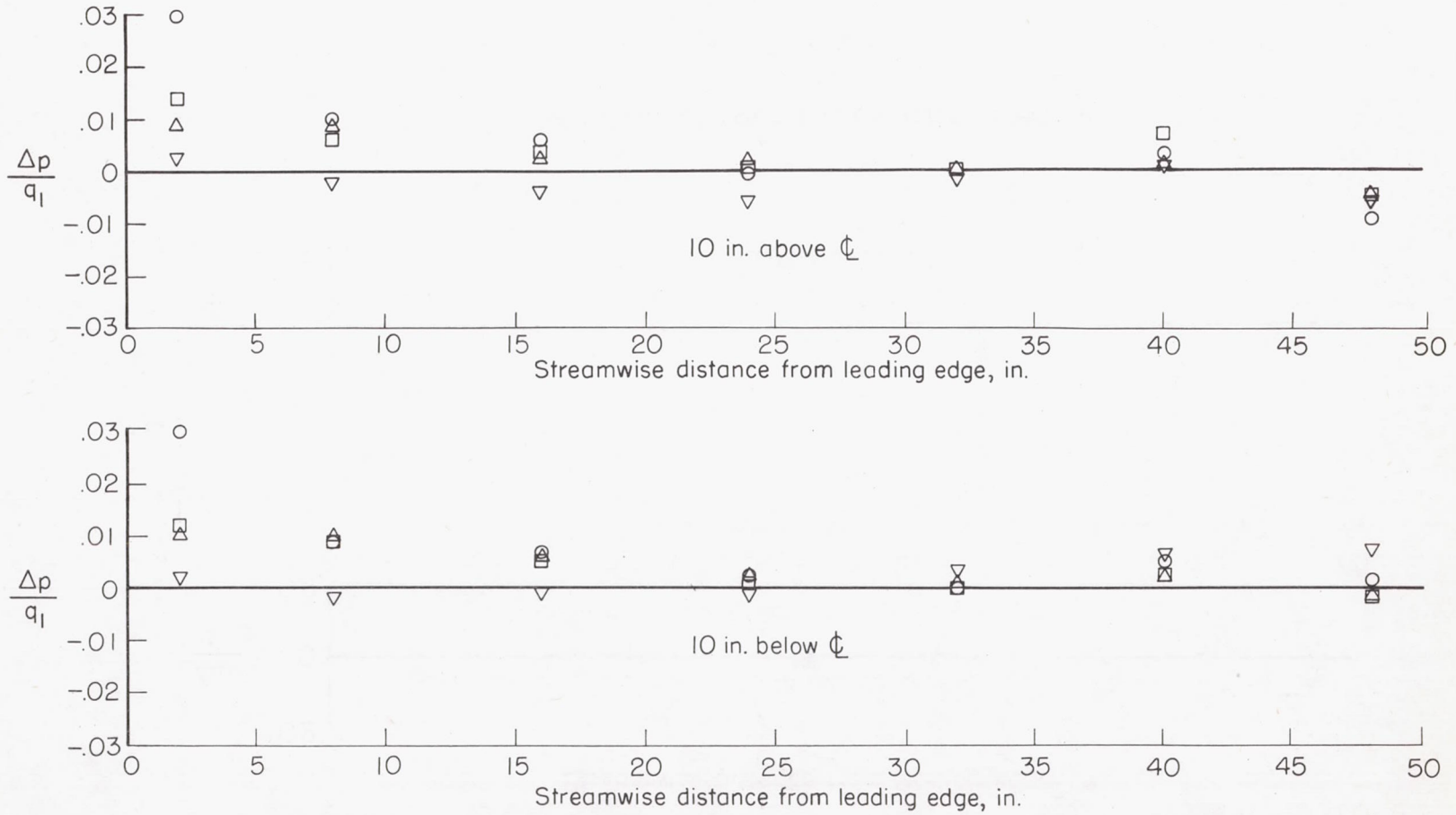

(b) Flat plate yawed 30°.

Figure 13.- Continued.

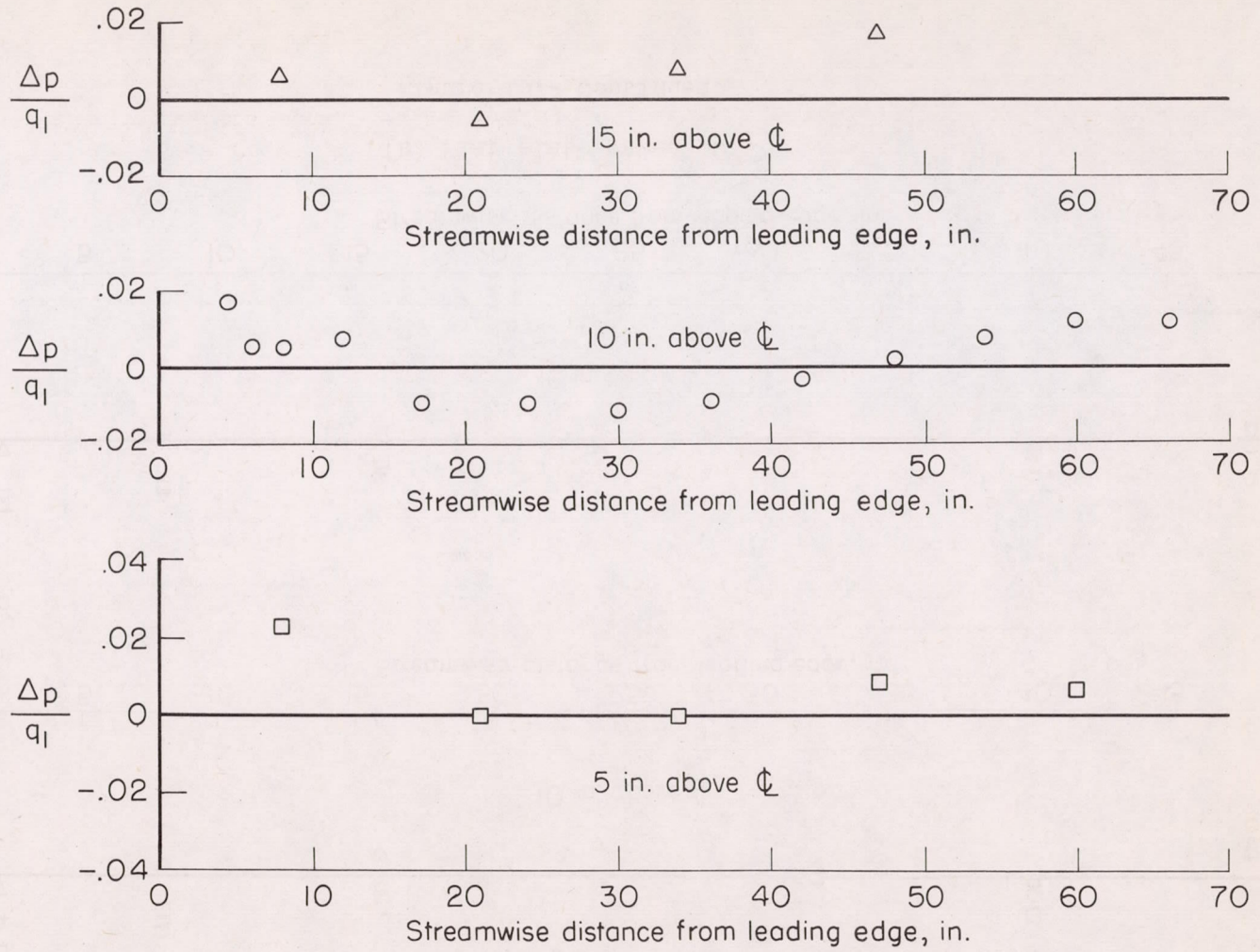

(c) Flat plate yawed 45°.

Figure 13.- Concluded.

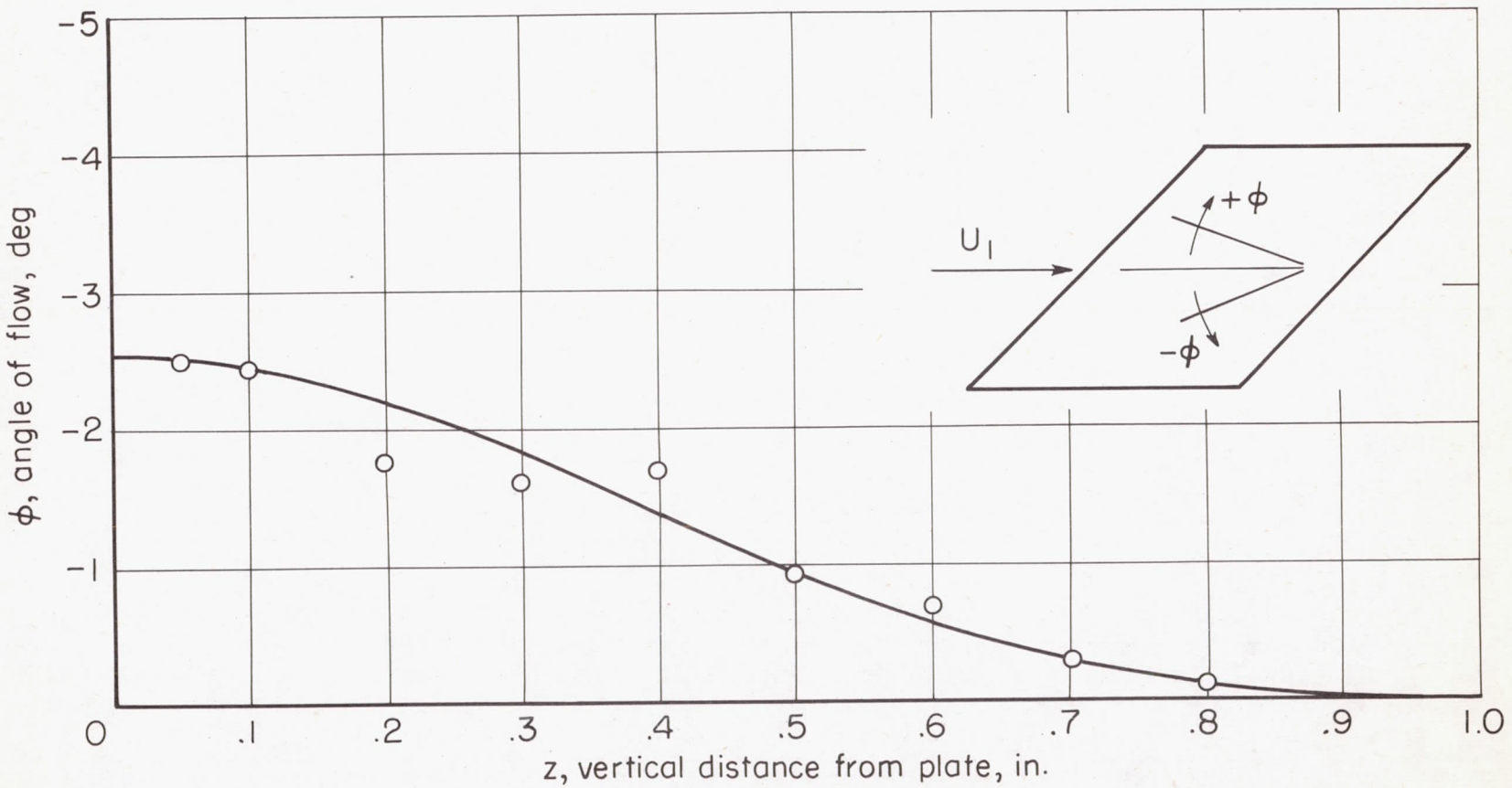

Figure 14.- Flow-direction profile taken at station. ξ = 36 inches, η = 15 inches; Λ = 45°; Re_1 = 250,000 per foot. The symbol λ represents relative flow deflection in the y-direction.

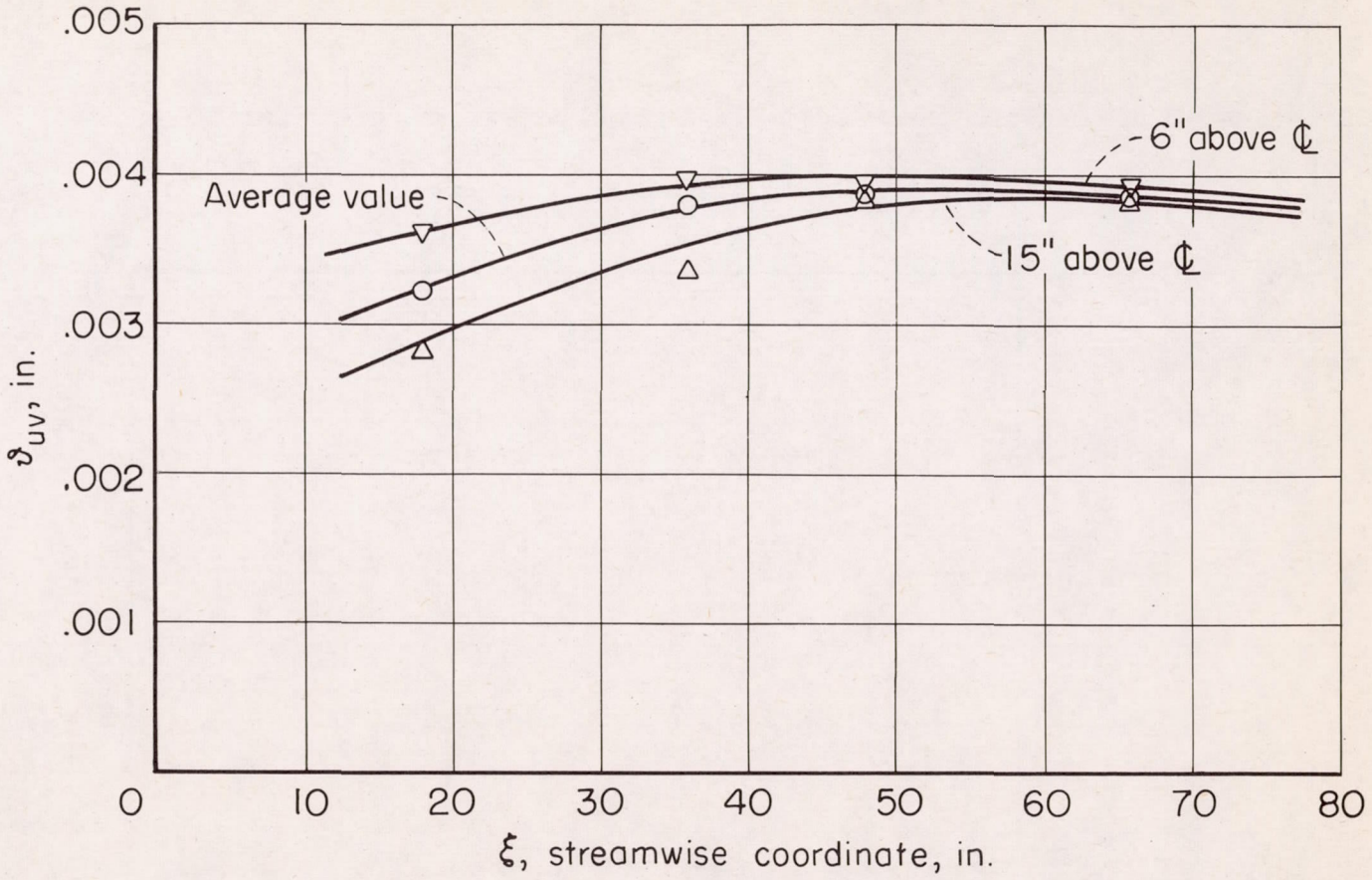

Figure 15.- Streamwise distribution of mixed momentum thickness. Re_1 = 250,000 per foot.

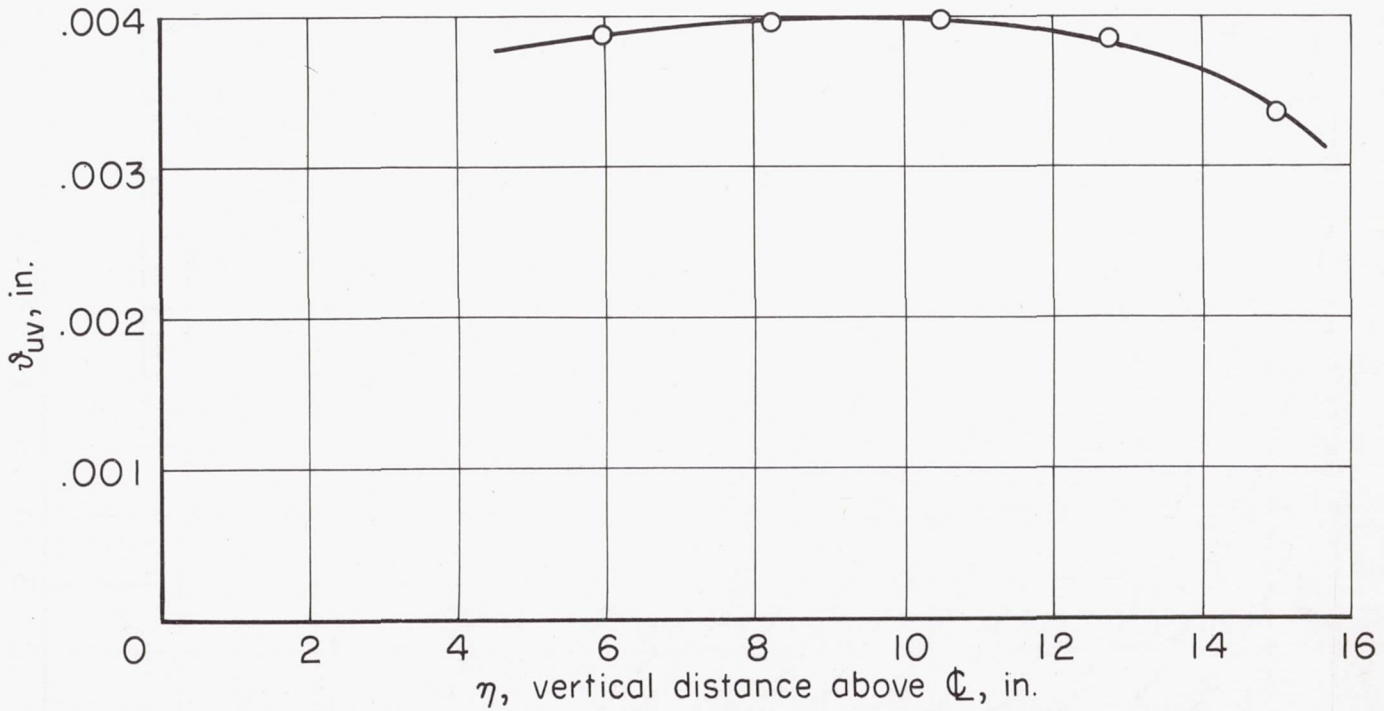

Figure 16.- Spanwise distribution of mixed momentum thickness taken 36 inches from leading edge. Re_1 = 250,000 per foot.

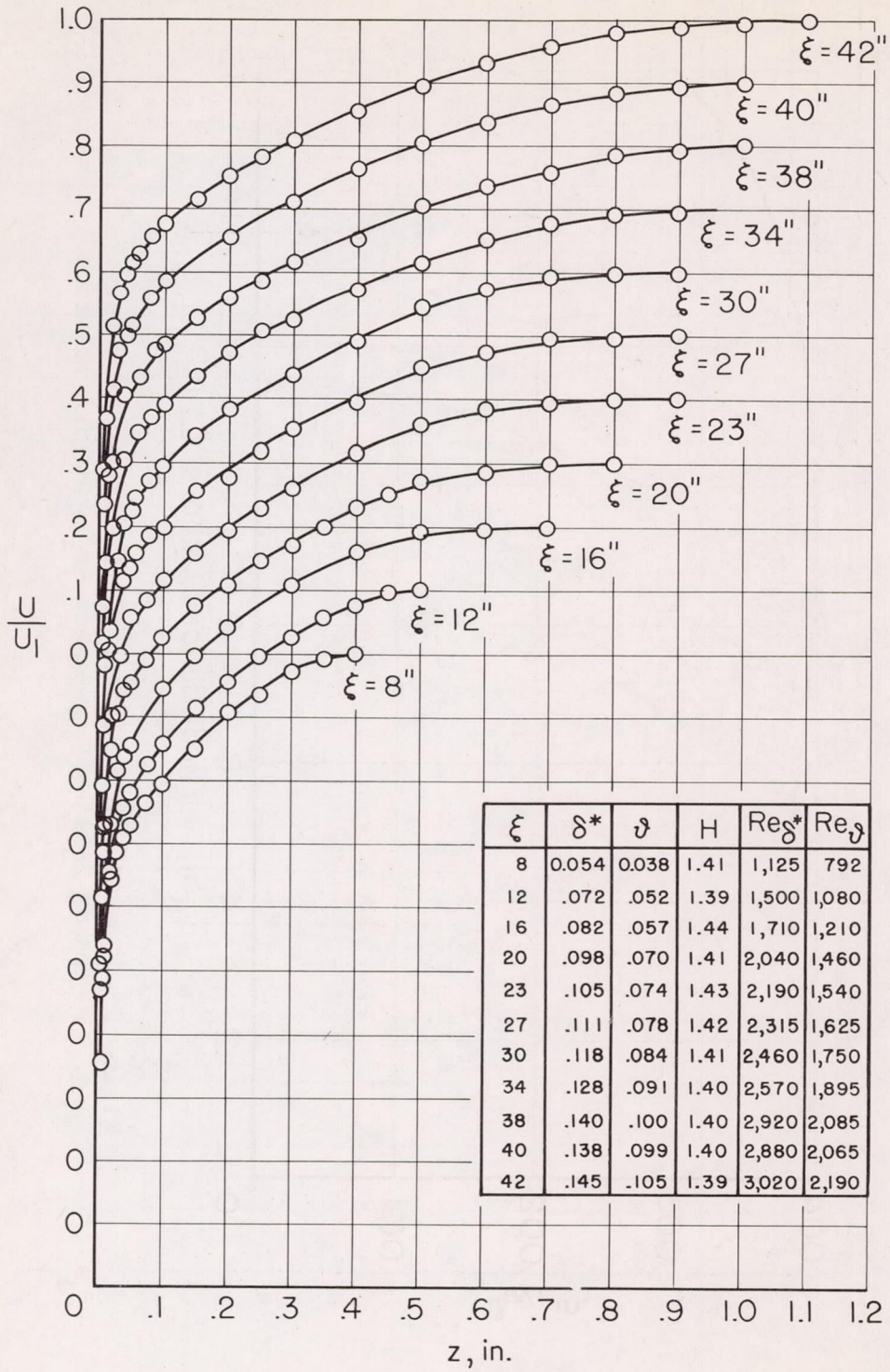

ξ	δ*	ϑ	H	Re_{δ^*}	Re_{ϑ}
8	0.054	0.038	1.41	1,125	792
12	.072	.052	1.39	1,500	1,080
16	.082	.057	1.44	1,710	1,210
20	.098	.070	1.41	2,040	1,460
23	.105	.074	1.43	2,190	1,540
27	.111	.078	1.42	2,315	1,625
30	.118	.084	1.41	2,460	1,750
34	.128	.091	1.40	2,570	1,895
38	.140	.100	1.40	2,920	2,085
40	.138	.099	1.40	2,880	2,065
42	.145	.105	1.39	3,020	2,190

(a) Unyawed flat plate.

Figure 17.- Boundary-layer profile. Re_1 = 250,000 per foot.

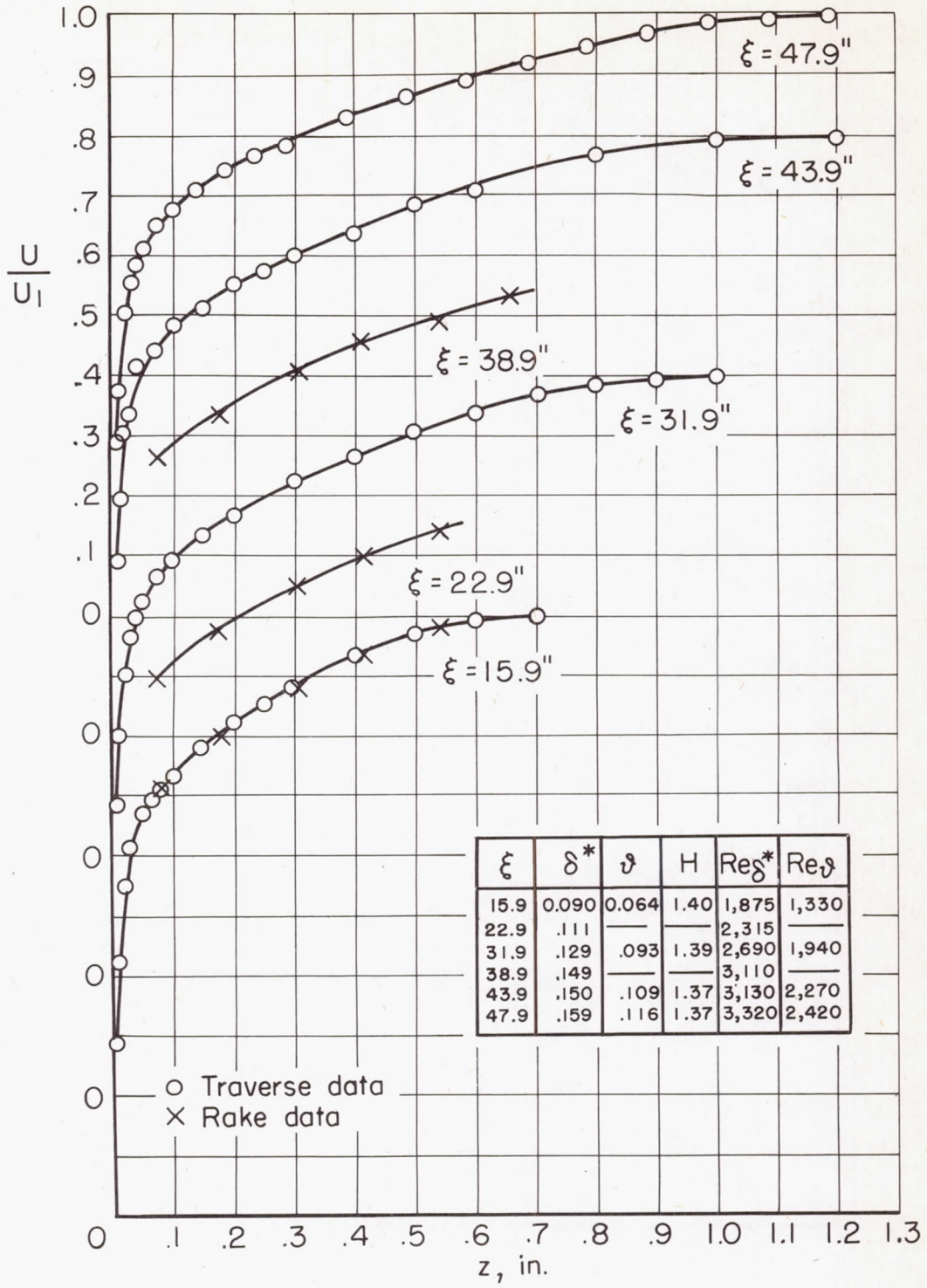

ξ	δ*	ϑ	H	Reδ*	Reϑ
15.9	0.090	0.064	1.40	1,875	1,330
22.9	.111	—	—	2,315	—
31.9	.129	.093	1.39	2,690	1,940
38.9	.149	—	—	3,110	—
43.9	.150	.109	1.37	3,130	2,270
47.9	.159	.116	1.37	3,320	2,420

(b) Flat plate yawed 30°.

Figure 17.- Continued.

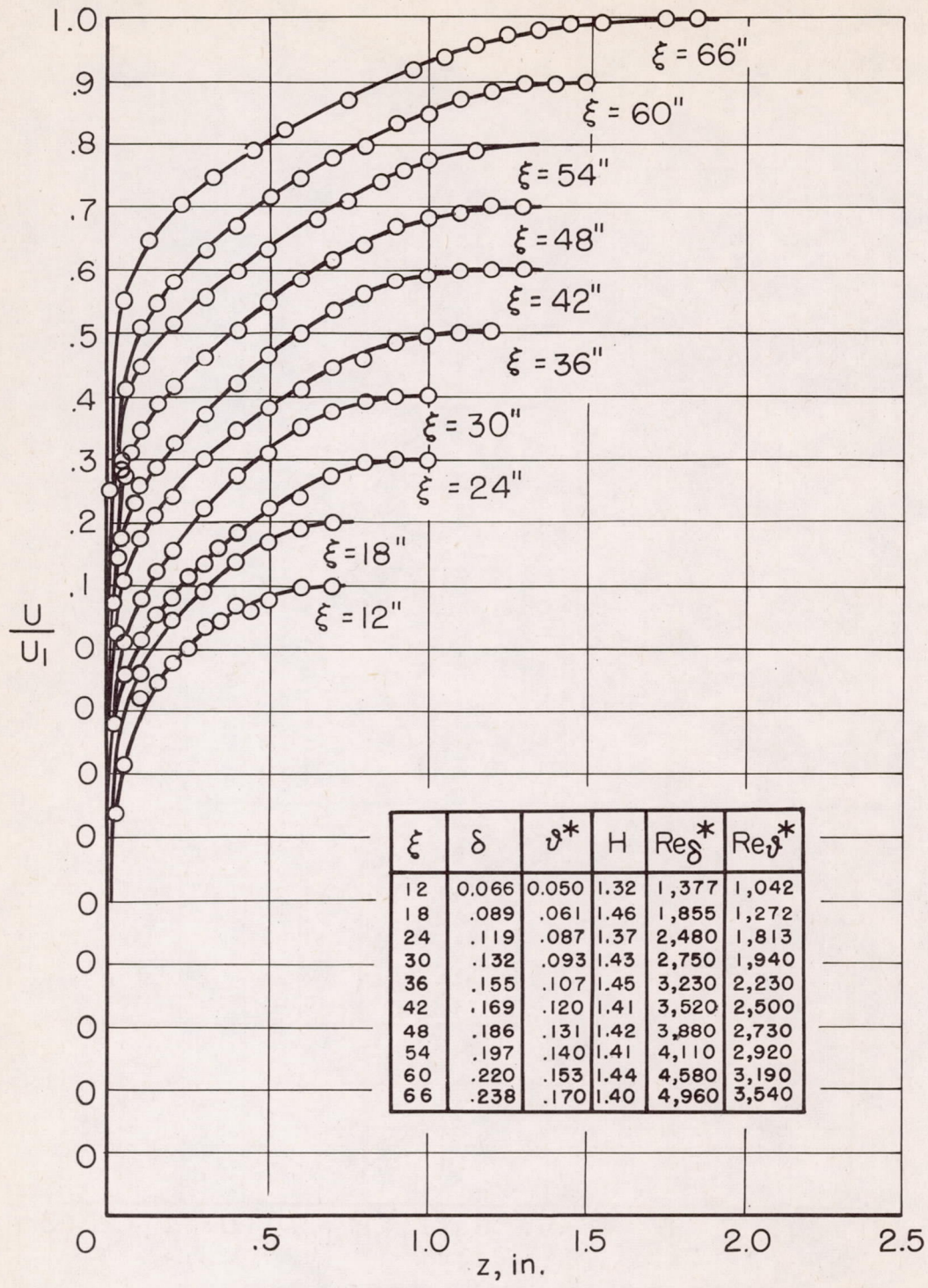

ξ	δ	ϑ*	H	Reδ*	Reϑ*
12	0.066	0.050	1.32	1,377	1,042
18	.089	.061	1.46	1,855	1,272
24	.119	.087	1.37	2,480	1,813
30	.132	.093	1.43	2,750	1,940
36	.155	.107	1.45	3,230	2,230
42	.169	.120	1.41	3,520	2,500
48	.186	.131	1.42	3,880	2,730
54	.197	.140	1.41	4,110	2,920
60	.220	.153	1.44	4,580	3,190
66	.238	.170	1.40	4,960	3,540

(c) Flat plate yawed 45°.

Figure 17.- Concluded.

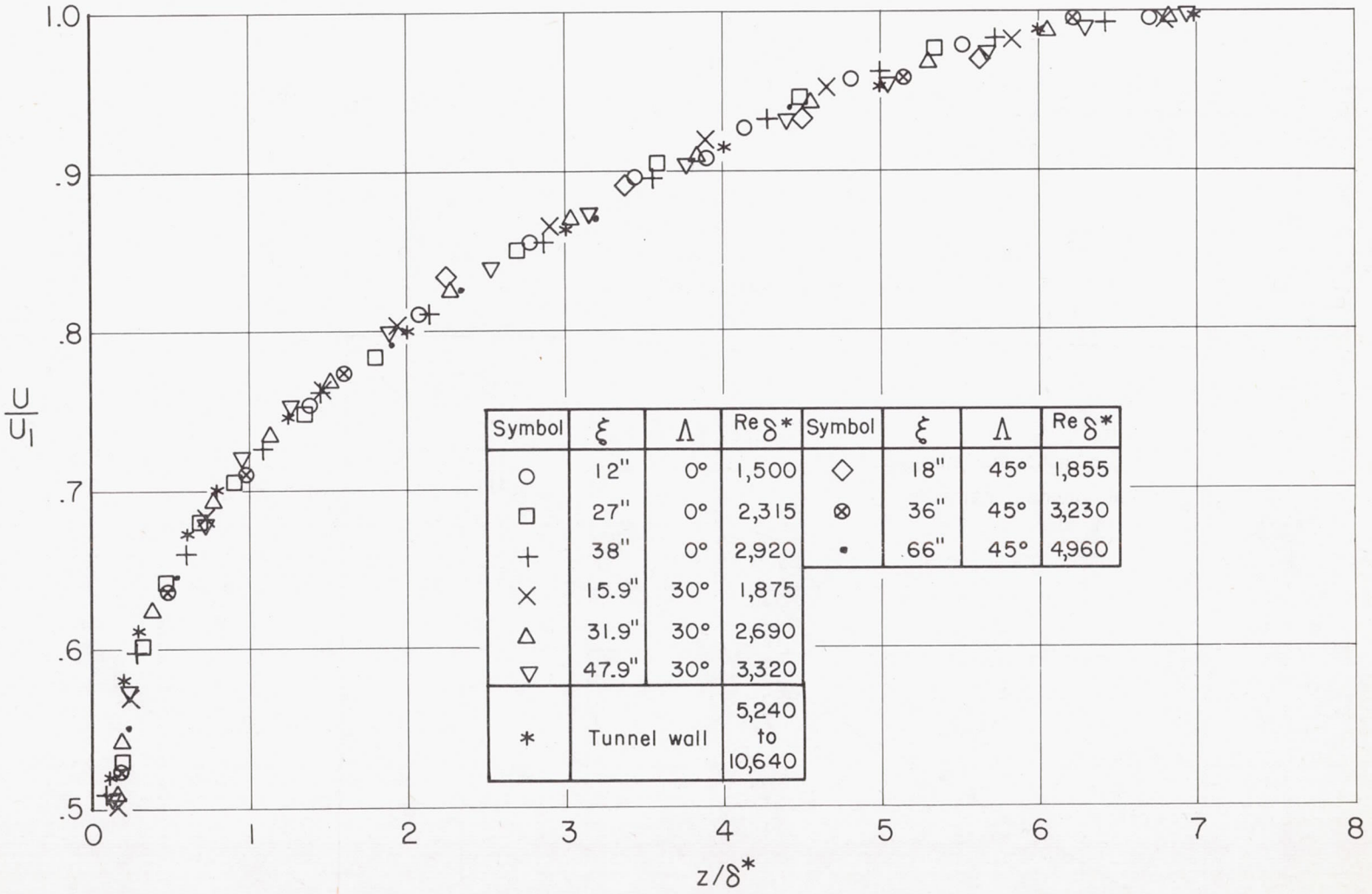

Symbol	ξ	Λ	$Re\,\delta^*$	Symbol	ξ	Λ	$Re\,\delta^*$
○	12"	0°	1,500	◇	18"	45°	1,855
□	27"	0°	2,315	⊗	36"	45°	3,230
+	38"	0°	2,920	•	66"	45°	4,960
×	15.9"	30°	1,875				
△	31.9"	30°	2,690				
▽	47.9"	30°	3,320				
*	Tunnel wall		5,240 to 10,640				

Figure 18.- Nondimensional velocity profiles. Zero pressure gradient.

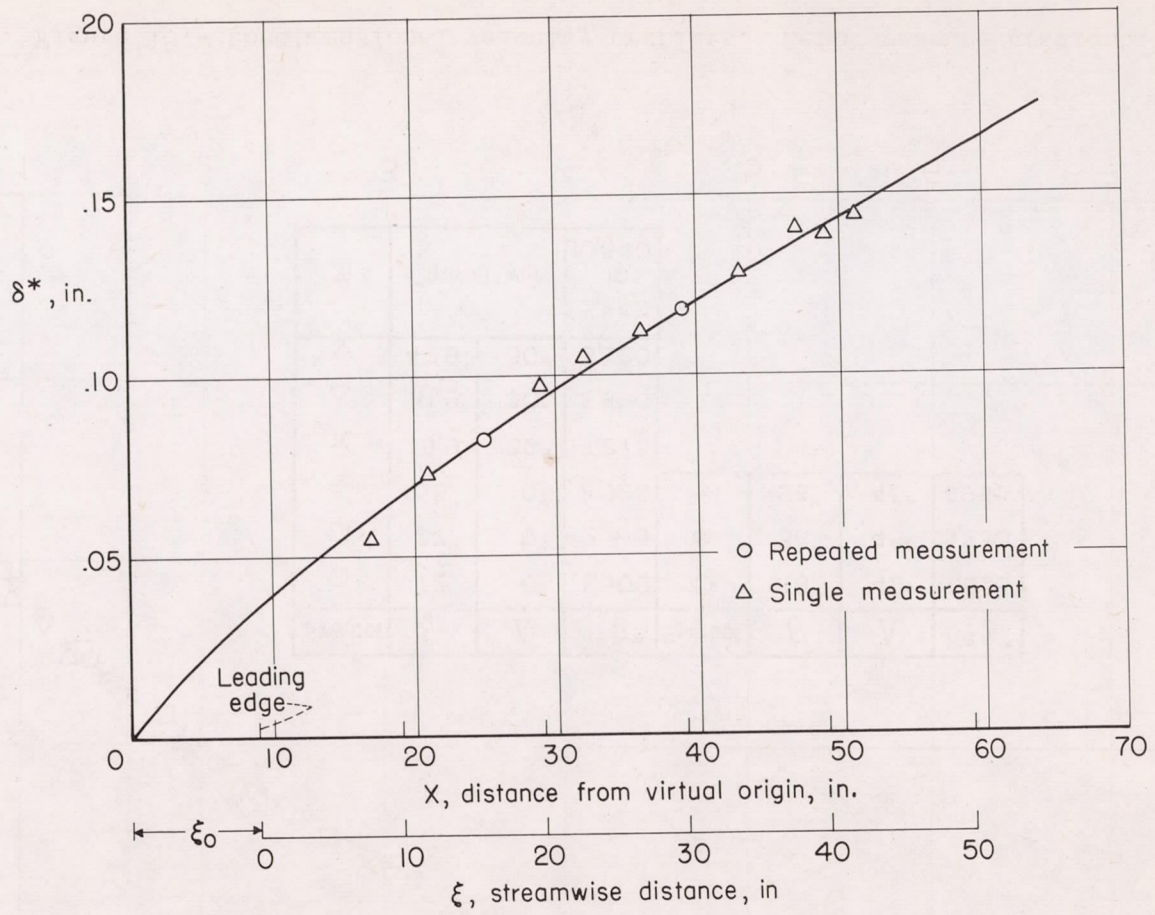

Figure 19.- Determination of ξ_o. Unyawed flat plate. $\delta^* = \dfrac{0.046(\xi + \xi_o)}{(Re)^{1/5}}$;

$$Re = \frac{(\xi + \xi_o)U_1}{\nu}.$$

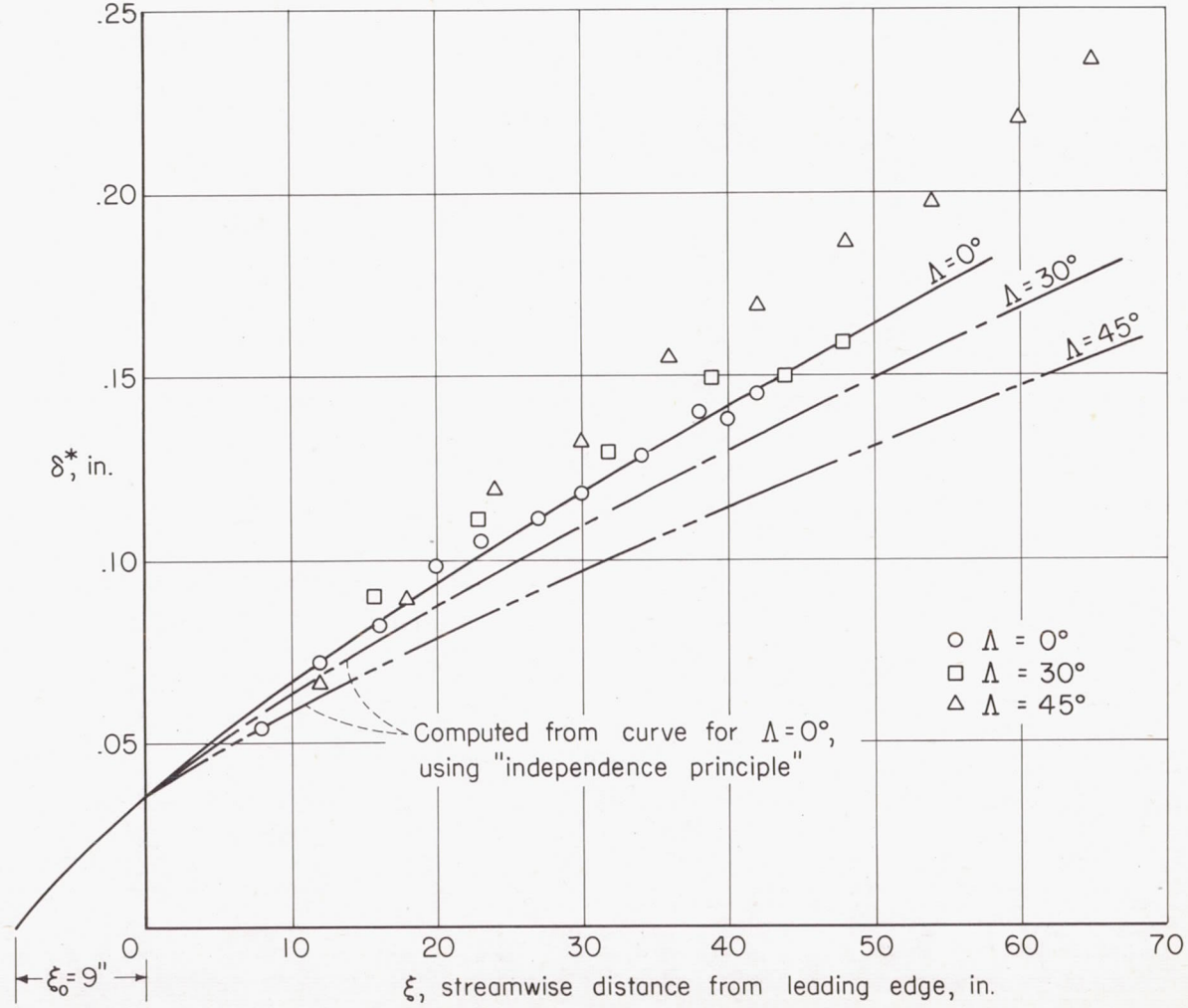

(a) ξ_o dependent on streamwise flow (constant).

Figure 20.- Boundary-layer growth. Re_1 = 250,000 per foot.

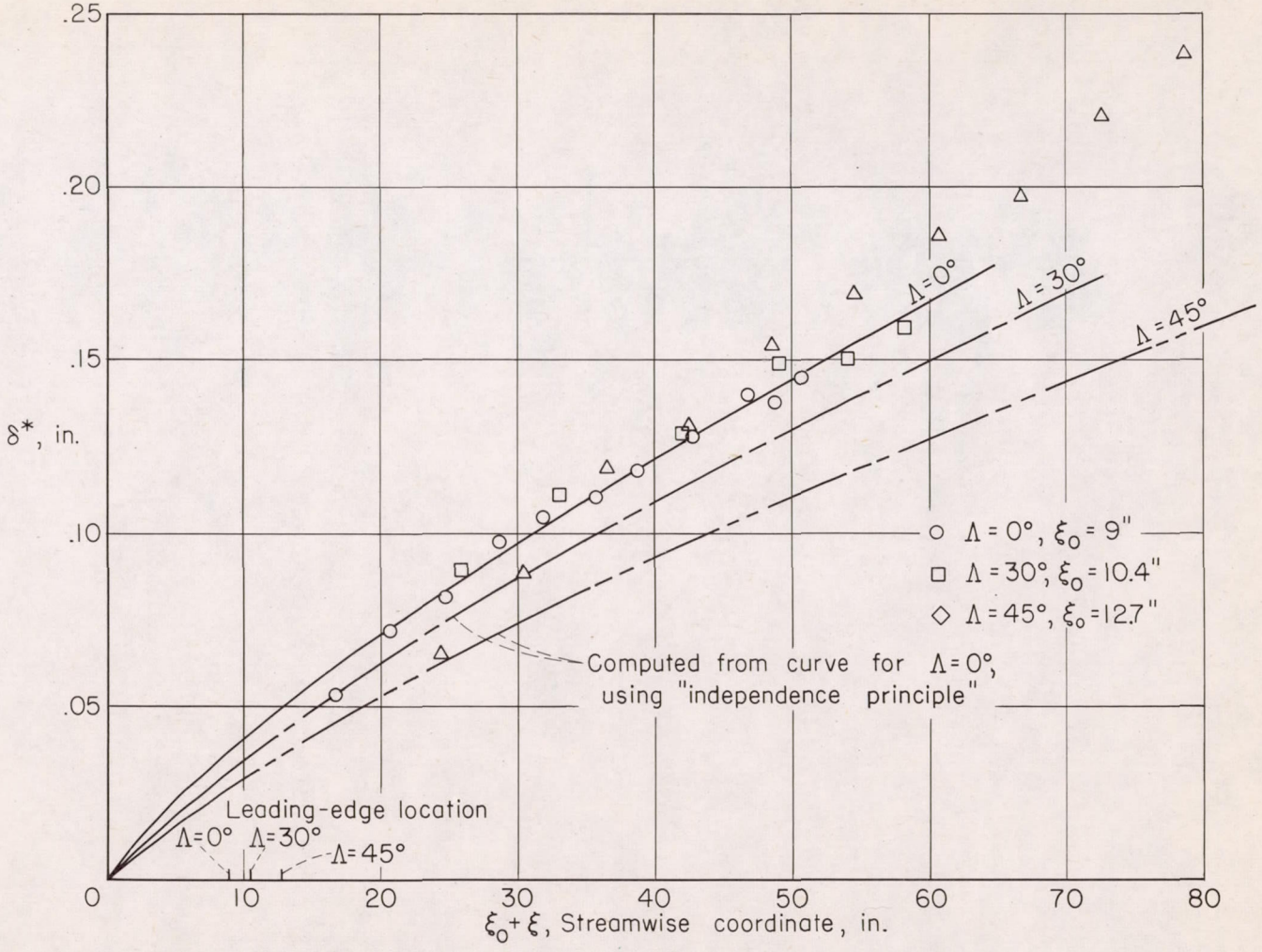

(b) ξ_o dependent on chordwise flow.

Figure 20.- Concluded.

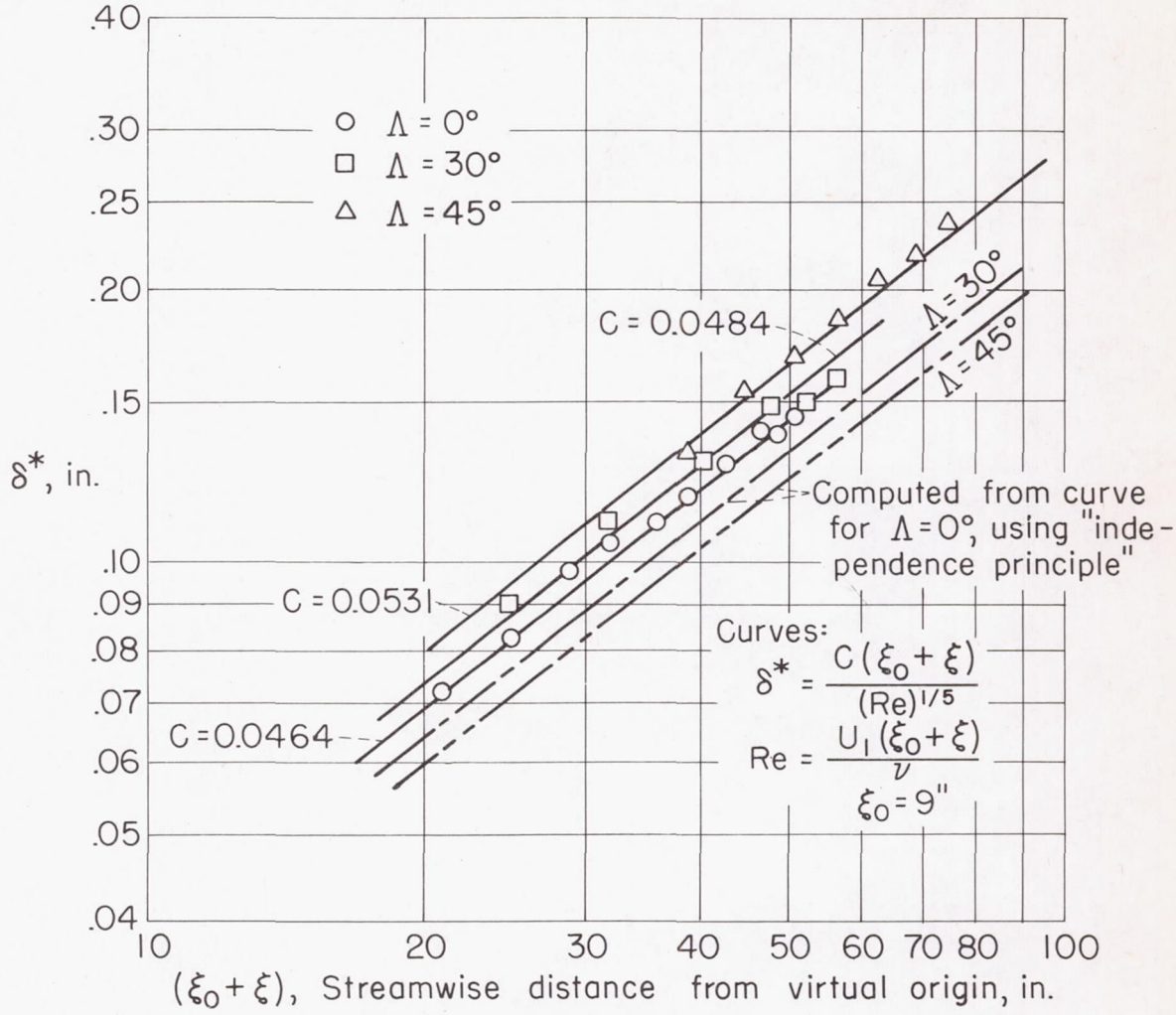

(a) Data presented in figure 20(a).

Figure 21.- Logarithmic plot of boundary-layer growth. Re_1 = 250,000 per foot.

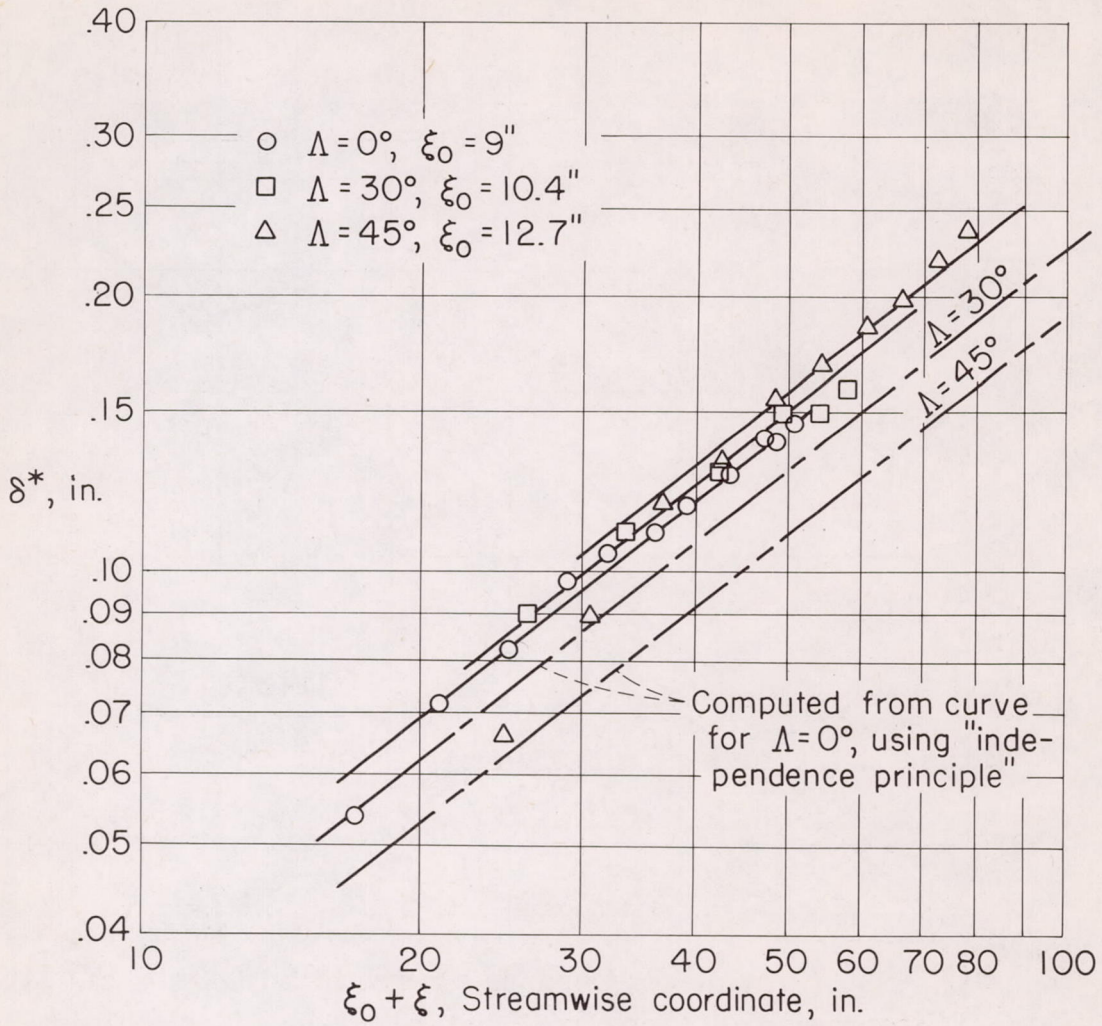

(b) Data presented in figure 20(b).

Figure 21.- Concluded.

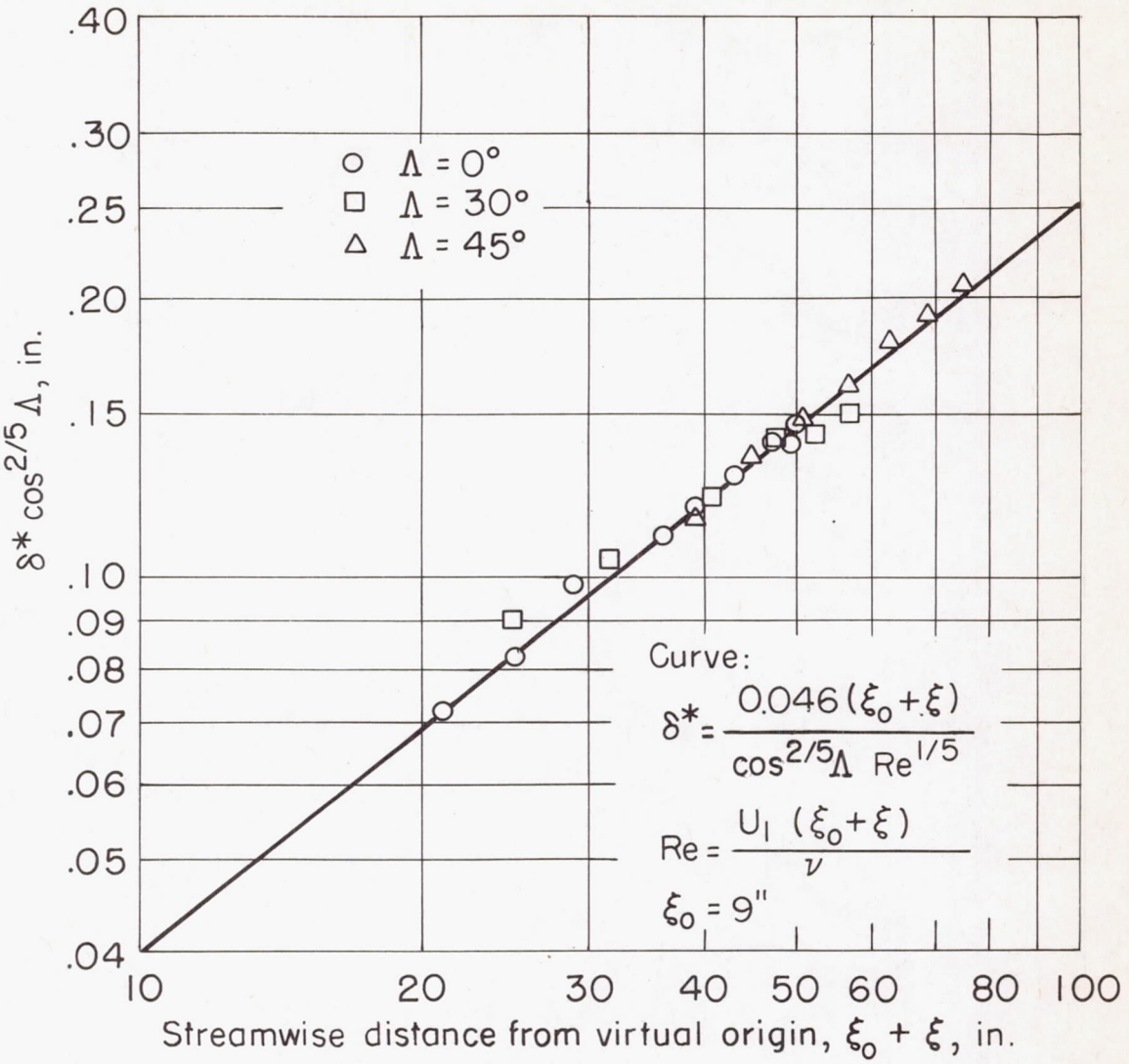

(a) Logarithmic plot.

Figure 22.- Boundary-layer growth obtained by using empirical $\cos^{2/5}\Lambda$ factor. Re_1 = 250,000 per foot.

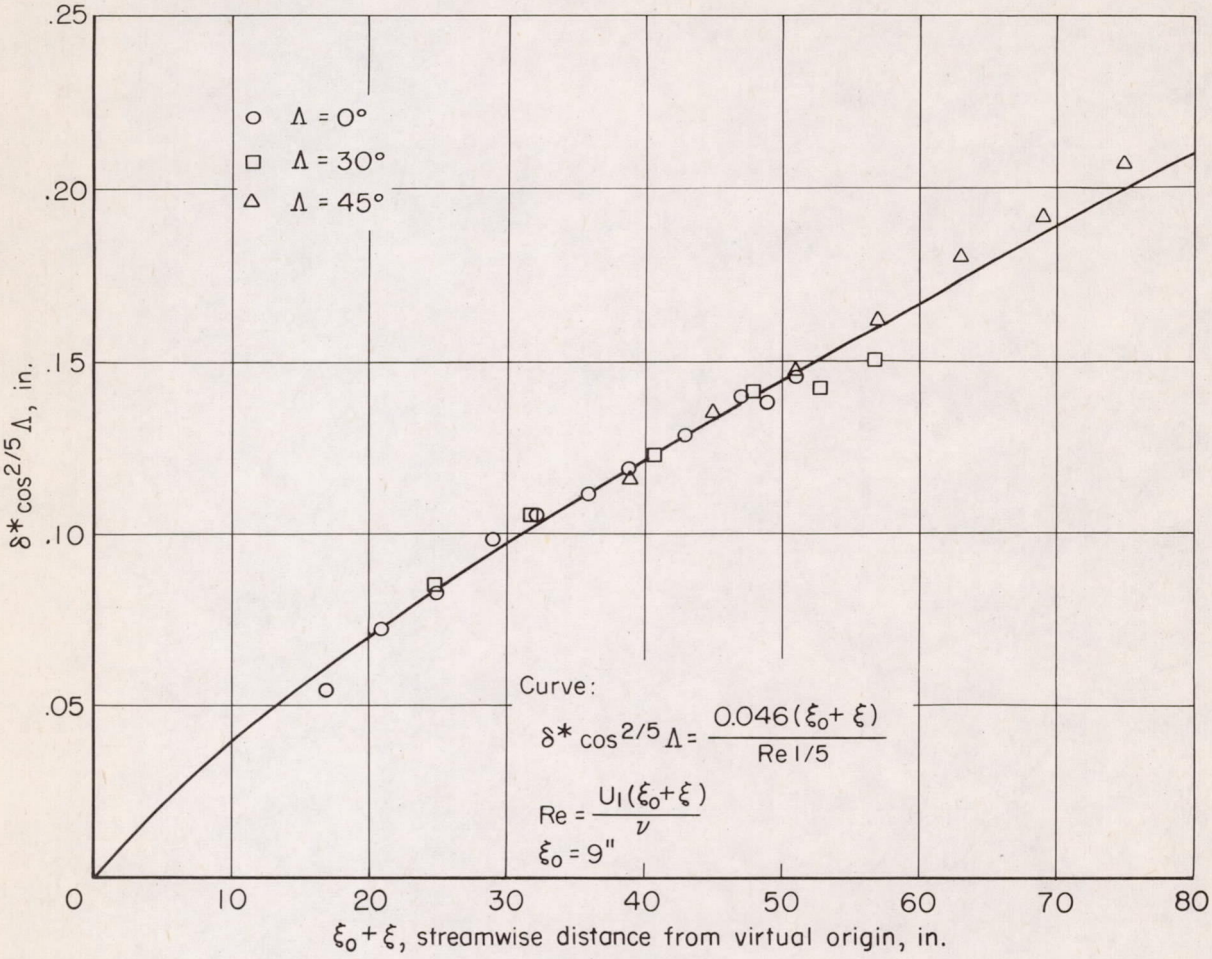

(b) Cartesian plot.

Figure 22.- Concluded.

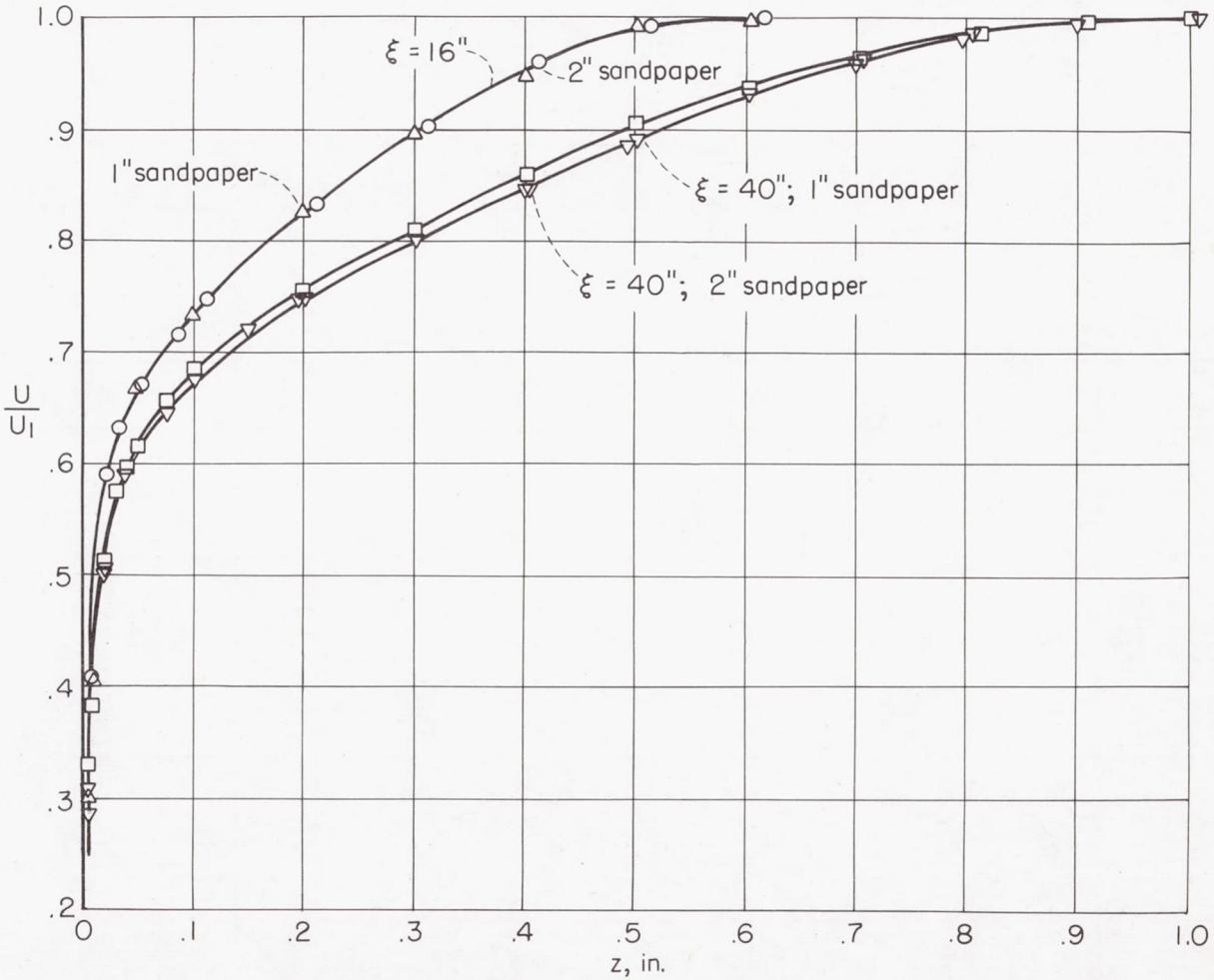

Figure 23.- Effect of sandpaper width on boundary-layer thickness on unyawed flat plate. Re = 250,000 × ξ (ξ in feet); for ξ = 40 inches, $\frac{\delta^*(\text{2 inches sandpaper})}{\delta^*(\text{1 inch sandpaper})} = 1.04$.

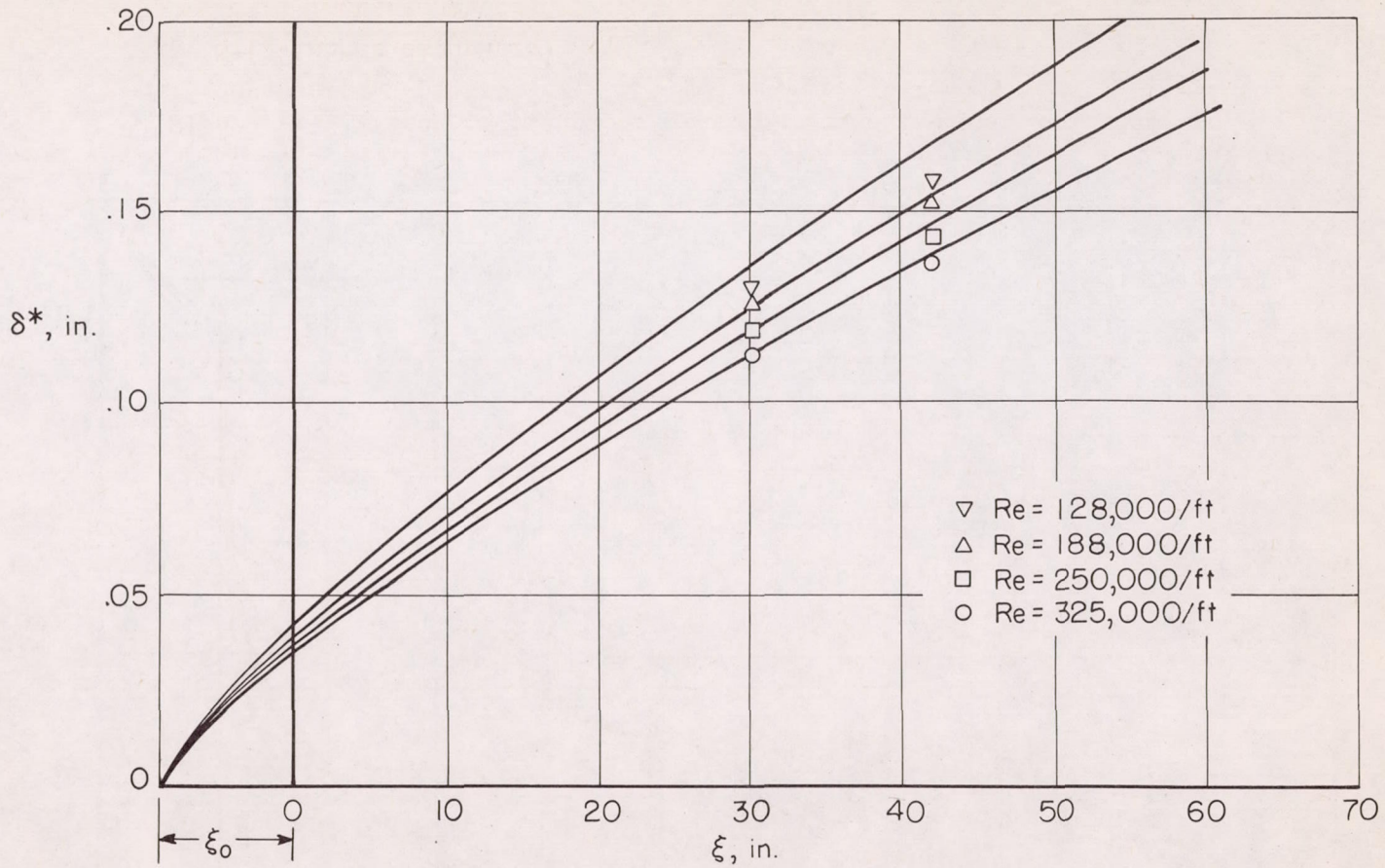

Figure 24.- Effect of Reynolds number change on virtual-origin distance. Unyawed flat plate. $\delta^* = \frac{0.046(\xi + \xi_o)}{Re^{1/5}}$; $Re = \frac{(\xi + \xi_o)U_1}{\nu}$; curves computed assuming $\xi_o = 9$ inches.

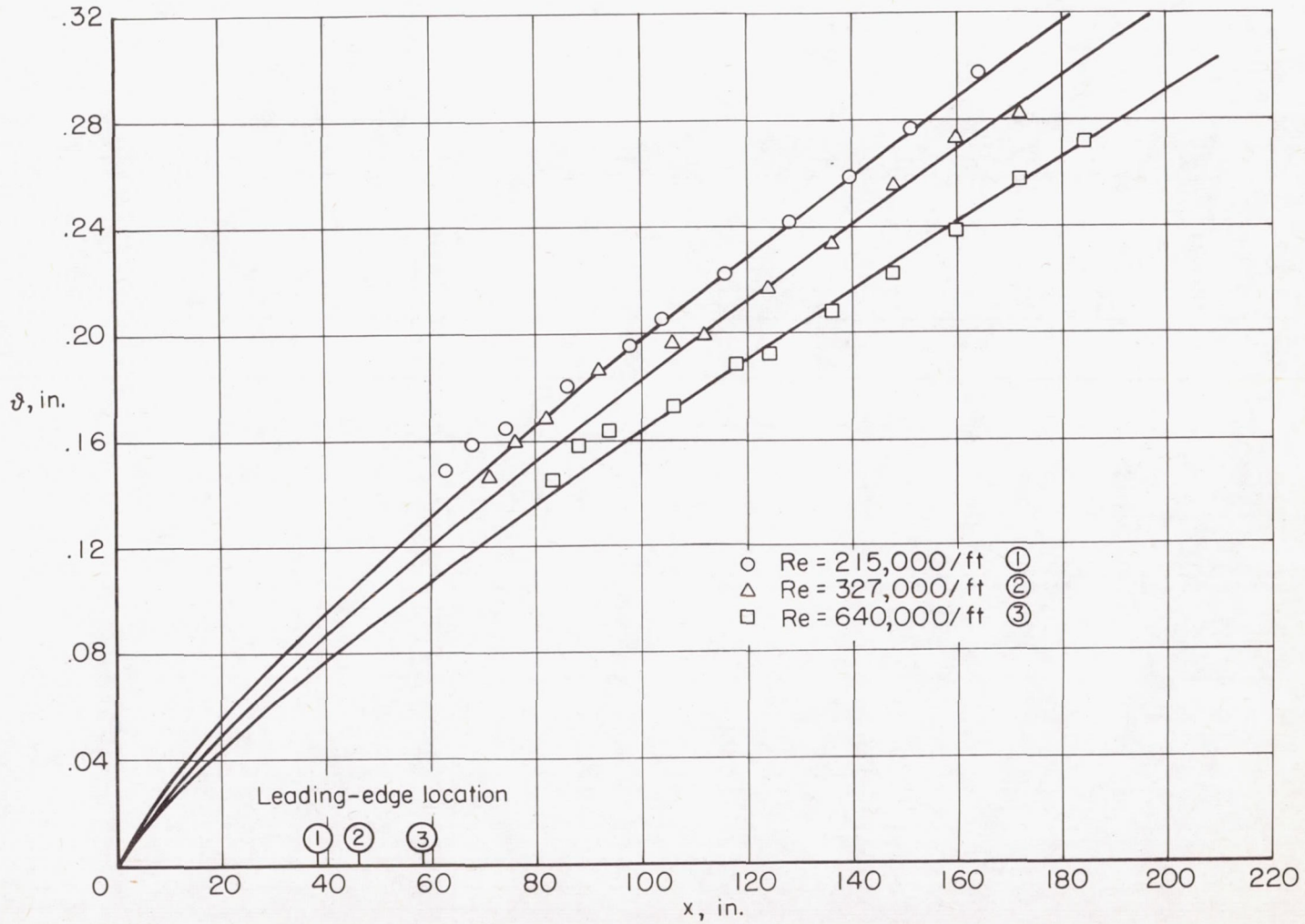

Figure 25.- Virtual-origin location. Data obtained from reference 4. 24-inch no. 16 floor sanding paper at leading edge.

$$x^{1/2} = 5.85\vartheta^{1/2} \log(2\,Re_{\vartheta}).$$

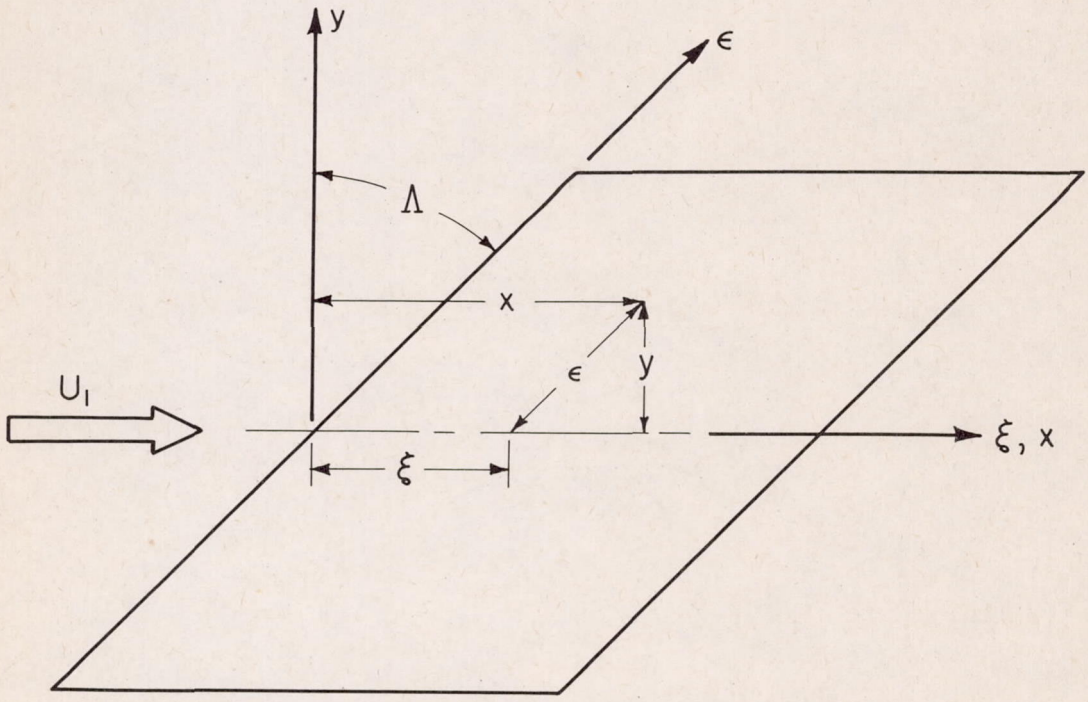

Figure 26.- Skewed coordinate system used in evaluating three-dimensional X-momentum derivatives.